



THE UNIVERSITY *of* EDINBURGH

Edinburgh Research Explorer

Evolution of arboreality and fossoriality in squirrels and aplodontid rodents: Insights from the semicircular canals of fossil rodents

Citation for published version:

Bhagat, R, Bertrand, OC & Silcox, MT 2021, 'Evolution of arboreality and fossoriality in squirrels and aplodontid rodents: Insights from the semicircular canals of fossil rodents', *Journal of Anatomy*, pp. 96-112. <https://doi.org/10.1111/joa.13296>

Digital Object Identifier (DOI):

[10.1111/joa.13296](https://doi.org/10.1111/joa.13296)

Link:

[Link to publication record in Edinburgh Research Explorer](#)

Document Version:

Peer reviewed version

Published In:

Journal of Anatomy

General rights

Copyright for the publications made accessible via the Edinburgh Research Explorer is retained by the author(s) and / or other copyright owners and it is a condition of accessing these publications that users recognise and abide by the legal requirements associated with these rights.

Take down policy

The University of Edinburgh has made every reasonable effort to ensure that Edinburgh Research Explorer content complies with UK legislation. If you believe that the public display of this file breaches copyright please contact openaccess@ed.ac.uk providing details, and we will remove access to the work immediately and investigate your claim.



1 **Evolution of arboreality and fossoriality in squirrels and aplodontid rodents:**
2 **insights from the semicircular canals of fossil rodents**

3 **Short running page heading:** Semicircular canals of extant and extinct rodents

4

5 Raj Bhagat^{1*}, Ornella C. Bertrand², Mary T. Silcox¹

6

7

8 ¹Department of Anthropology, University of Toronto Scarborough, Toronto, ON M1C 1A4,
9 Canada

10

11 ²School of GeoSciences, University of Edinburgh, Grant Institute, Edinburgh, Scotland, UK

12

13

14 *Corresponding author

15 raj.bhagat@mail.utoronto.ca

16

17 **Short abstract:** Here we employ two methods of reconstructing locomotor agility from the
18 semicircular canals (SCCs) of fossil rodents: radius of curvature dimensions and SCC
19 orthogonality. Radius of curvature dimensions provide compelling evidence that arboreality was
20 likely an ancestral trait for the Sciuroidea clade, and that early aplodontids were more arboreal
21 than their burrowing descendants.

22 **Abstract** – Reconstructing locomotor behaviour for fossil animals is typically done with
23 postcranial elements. However, for species only known from cranial material, locomotor
24 behaviour is difficult to reconstruct. The semicircular canals (SCCs) in the inner ear provide
25 insight into an animal's locomotor agility. A relationship exists between the size of the SCCs
26 relative to body mass and the jerkiness of an animal's locomotion. Additionally, studies have
27 also demonstrated a relationship between SCC orthogonality and angular head velocity. Here we
28 employ two metrics for reconstructing locomotor agility, radius of curvature dimensions and
29 SCC orthogonality, in a sample of twelve fossil rodents from the families Ischyromyidae,
30 Sciuridae, and Aplodontidae. The method utilizing radius of curvature dimensions provided a
31 reconstruction of fossil rodent locomotor behaviour that is more consistent with previous studies
32 assessing fossil rodent locomotor behaviour compared to the method based on SCC
33 orthogonality. Previous work on ischyromyids suggests that this group displayed a variety of
34 locomotor modes. Members of Paramyinae and Ischyromyinae have relatively smaller SCCs and
35 are reconstructed to be relatively slower compared to members of Reithroparamyinae. Early
36 members of the Sciuroidea clade including the sciurid *Cedromus wilsoni* and the aplodontid
37 *Prosciurus relictus* are reconstructed to be more agile than ischyromyids, in the range of extant
38 arboreal squirrels. This reconstruction supports previous inferences that arboreality was likely an
39 ancestral trait for this group. Derived members of Sciuridae and Aplodontidae vary in agility
40 scores. The fossil squirrel *Protosciurus* cf. *rachelae* is inferred from postcranial material as
41 arboreal, which is in agreement with its high agility, in the range of extant arboreal squirrels. In
42 contrast, the fossil aplodontid *Mesogaulus paniensis* has a relatively low agility score, similar to
43 the fossorial *Aplodontia rufa*, the only living aplodontid rodent. This result is in agreement with

44 its postcranial reconstruction as fossorial and with previous indications that early aplodontids
45 were more arboreal than their burrowing descendants.

46 **Keywords:** inner ear, adaptation, Ischyromidae, Sciuroidea, locomotion, agility

47

For Peer Review Only

48 **Introduction**

49 The semicircular canals (SCCs) are housed in the petrosal bone (or petrous portion of the
50 temporal) and are composed of three passageways (i.e., anterior, posterior and lateral SCCs) that
51 are at approximately 90 degrees to one another (Spoor and Zonneveld, 1998). The SCCs are a
52 part of the bony labyrinth which contains the soft tissue sacs and ducts that make up the
53 membranous labyrinth (Lewis et al., 1985). The membranous ducts are filled with endolymph
54 fluid, which, under inertial drag from movement, aid in detecting angular head accelerations and
55 contribute to the stabilization of gaze during locomotion (Spoor and Zonneveld, 1998; Hullar,
56 2006; Berlin et al., 2013). Due to the concealed nature of the inner ear in the petrosal bone,
57 studying its morphology proved to be difficult for early anatomists and required time-consuming
58 and destructive techniques (as discussed in Spoor and Zonneveld, 1995). However, the increased
59 use of X-ray computed tomography (CT) has provided an effective way to non-destructively
60 measure and analyze inner ear morphology in extant and extinct specimens. Today, high
61 resolution X-ray micro-computed tomography is commonly used to study SCC dimensions and
62 morphology in detail (e.g., Spoor and Zonneveld 1995; Lebrun et al., 2010; Gunz et al., 2012;
63 Malinzak et al., 2012; Berlin et al., 2013; Billet et al., 2015; Pfaff et al., 2015; Grohé et al., 2016;
64 Mennecart and Costeur, 2016; Bernardi and Couette, 2017). Although CT data do not allow for
65 characterization of the membranous labyrinth, the close relationship between the bony and
66 membranous structures suggests that measurements of the bony labyrinth will mirror the
67 functionally relevant parameters of the membranous structures. Using this approach also allows
68 for the collection of data that is directly comparable to measurements of fossil specimens, in
69 which the membranous labyrinth is not preserved.

70 Due to their relationship to vestibular sensitivity and angular head movements, the
71 morphology of the SCCs is closely associated with an animal's locomotor behaviour (Spoor and
72 Zonneveld, 1995, 1998; Yang and Hullar, 2007; Malinzak et al., 2012). Although in vertebrate
73 paleontology, postcrania (e.g., long bones, pelvis, calcanei etc.) are typically used to reconstruct
74 locomotor behaviour, many species are known only from cranial material. In particular, the
75 petrosal bone preserves well in the fossil record because of its high density. Analyzing the
76 relationship between SCC morphology and agility level (i.e., jerkiness of movement) or other
77 aspects of locomotor behaviour in extant taxa can therefore help paleontologists make inferences
78 about fossil species known from petrosals but not postcranial remains (e.g., Walker et al., 2008;
79 Silcox et al., 2009; Orliac et al., 2012; Ryan et al., 2012; Billet et al., 2015; Ruf et al., 2016;
80 Bernardi and Couette, 2017).

81 Three main methodologies have been proposed to relate data from the SCCs to aspects of
82 locomotor behaviour in extant taxa (Table 1). To date, the largest and most diverse group of
83 extant taxa has been assessed by Spoor et al. (2007). The authors ranked SCC sensitivity based
84 on agility scores derived from field observations and video footage. Agility scores were ranked
85 on a scale from 1-6 with 1 being extremely slow and 6 being fast. Their results show that animals
86 with larger average SCC radii of curvature relative to body size have faster, jerkier locomotion
87 compared to animals with smaller canals (Spoor et al., 2007). This relationship makes sense in
88 light of work that has established a link between the relative size of the SCCs and their
89 sensitivity (Spoor and Zonneveld, 1998; Yang and Hullar, 2007; Cox and Jeffery, 2010). The
90 dataset provided by Spoor and colleagues (2007) has frequently been used to reconstruct
91 locomotor behaviour from fossils (e.g., primates [Walker et al., 2008; Silcox et al., 2009; Ryan et
92 al., 2012; Bernardi and Couette, 2017], leptictids [Ruf et al., 2016], artiodactyls [Orliac et al.,

93 2012], xenarthrans [Billet et al., 2015], and early placental mammals [Cameron et al., 2019;
94 Bertrand et al., 2020]). This is likely because of its large size and extensive taxonomic coverage
95 (Table 1). Also, despite the rather qualitative approach to assessing agility, it relates the SCC
96 radii to an aspect of behaviour that can be clearly understood with respect to a species'
97 locomotor repertoire.

98 Pfaff et al. (2015) conducted a morphometric analysis of the SCCs using scaled data
99 based on cranial measurements rather than body mass. Their sample included 50 taxa, mainly
100 from the squirrel-related clade (Sciuridae, Gliridae, and Aplodontidae; Table 1). As opposed to
101 using agility scores as a proxy for vestibular sensitivity, they calculated a measure of sensitivity
102 based on SCC dimensions. They found substantial differences between subterranean, flying and
103 gliding taxa. The vestibular sensitivity of the SCCs in fossorial sciurids was found to be higher
104 relative to arboreal and gliding taxa, based largely on variation in the SCC diameters. They
105 reasoned that the lessened sensory information flow during locomotion in flying and gliding taxa
106 may be necessary to prevent over stimulation of the vestibular system (Schutz et al., 2014; Pfaff
107 et al., 2015). The majority of their sample consisted of fossorial, arboreal and gliding taxa,
108 therefore limiting inferences using this method of the vestibular sensitivity of taxa with less
109 extreme locomotor behaviours (i.e., scansorial). Further investigation is still required to
110 understand how SCC diameter influences sensitivity in other taxa beyond the squirrel-related
111 clade. Additionally, measuring SCC diameter accurately is more challenging than measuring
112 canal radii or angles. As a very small measurement, it will be more impacted, as a percentage of
113 the measurement, by the threshold selected for the segmentation of the SCCs—this is a
114 byproduct of partial volume averaging, which leads to changes in the apparent outer edge of the
115 bone depending on the threshold used. Pfaff et al. (2015) acknowledge that they used different

116 threshold values in their manual segmentation process, but they did not consider the impact of
117 varying thresholds on this measurement, which means that they did not account for the fact that
118 different datasets would have different amounts of error introduced by partial voluming
119 averaging. These authors also did not consider the degree to which their approach to scaling their
120 measurements influenced their results.

121 As opposed to qualitatively assessing agility, Malinzak et al. (2012) directly measured
122 angular velocity magnitude (AVM) of head rotations as a variable representing vestibular
123 sensitivity in eleven strepsirrhine primates (Table 1). They found animals with more
124 orthogonally positioned SCCs had higher angular head velocities than those with less orthogonal
125 canals. Additionally, from analyzing angular head velocities with radii of curvature data from
126 Spoor et al. (2007), they found no relationship between the two. However, Malinzak et al. (2012)
127 had a small and not very diverse sample, either taxonomically, or in terms of the range of
128 locomotor behaviours represented (Table 1). In contrast, results from Berlin et al. (2013)
129 demonstrated that the radii of curvature (analyzed without angular velocity measurements) do in
130 fact influence vestibular sensitivity in their larger and more diverse sample. In addition, studies
131 using angular data to reconstruct locomotor behaviour in fossil taxa have shown a high degree of
132 within-species variability, leading to the reconstruction of an implausible range of different
133 behaviours for one species (Bernardi and Couette, 2017). This is in contrast to reconstructions
134 using the radii of curvature, which yielded much more consistent agility estimates (Bernardi and
135 Couette, 2017).

136 Here, we examine both the radii of curvature and degree of orthogonality of the SCCs for
137 twelve fossil species of rodents from Ischyromyidae, and Sciuroidea (Sciuridae + Aplodontidae;
138 Table 2). In spite of concerns about the applicability of the Malinzak et al. (2012) sample to

139 non-primate groups we included their approach, since it is the only dataset with quantitative
140 measures of angular velocity. The method from Pfaff et al. (2015) was not used for two reasons:
141 1. the lack of an error study demonstrating that small measurements such as the SCC diameter
142 can be accurately measured in diverse microCT datasets across varying thresholds and 2. the lack
143 of more behaviourally generalized rodents in their comparative sample, which is problematic when
144 assessing locomotor behaviour in the range of fossil taxa considered here.

145 Sciuridae includes 58 extant genera and 285 species (Burgin et al., 2018). Squirrels are
146 diverse in terms of locomotion, exhibiting terrestrial, scansorial, arboreal and gliding adaptations
147 (Koprowski et al., 2016). The oldest sciurid known from postcranial material, the late Eocene
148 *Douglassciurus jeffersoni* has been interpreted as arboreal (Emry and Thorington, 1982). During
149 the Oligocene and Miocene, squirrels rapidly invaded their modern-day ecological niches
150 (Mercer et al., 2003; Thorington et al., 2012). The sister-clade to Sciuridae, Aplodontidae, is
151 only represented by a single species today, *Aplodontia rufa*. In the past, this group was more
152 diverse, and was distributed across the Holarctic regions, being recovered from North America,
153 Europe and Asia (Hopkins, 2008). Fossil Aplodontidae have been inferred to have exhibited a
154 diverse array of behavioural locomotor types, with some specimens being reconstructed as
155 fossorial (e.g. aplodontines and mylagaulines), as burrowing (meniscomyines), and even as
156 having arboreal, squirrel-like adaptations (allomyines, prosciurines) based on postcranial and
157 cranial data (Hopkins, 2005; 2008). The family's earliest members display squirrel-like
158 adaptations, suggestive of arboreal and scansorial locomotor behaviour (Hopkins, 2005; 2008).

159 Ischyromyidae has been considered one of the most primitive rodent families (Korth,
160 1994) and has been discovered in North America (late Paleocene to early Eocene), Europe (early
161 to late Eocene), and Asia (Early Oligocene; Korth, 1994; Anderson, 2008). There is uncertainty

162 about the relationships within Ischyromyidae and with other rodent families. A comprehensive
163 analysis including representatives of all the various groups has yet to be published. Figure 1
164 illustrates the two most broadly supported hypotheses for the relationships among Ischyromyidae
165 and Sciuroidea. The only difference stems from the position of Reithroparamyinae, which might
166 either be more closely related to the Sciuroidea (Meng, 1990) or to Paramyinae (Asher et al.,
167 2019). The positions of the fossil sciuroids in Figure 1 are based on different studies (Korth and
168 Emry, 1991; Hopkins, 2008; Korth and Samuels, 2015), while the position of the extant
169 squirrels, and their relationship to *Aplodontia rufa*, is based on molecular phylogenies (Mercer et
170 al., 2003; Blanga-Kanfi et al., 2009; Churakov et al., 2010; Fabre et al., 2012).

171 Studies on postcranial anatomy reveal that Ischyromyidae had diverse lifestyles. The
172 early Eocene paramyine, *Paramys*, may have been scansorial, spending some time in the trees
173 and on the ground (Rose and Chinnery, 2004). Other members of this subfamily, *Pseudotomus*
174 (Middle Eocene) was larger, and probably fossorial (Dunn and Rasmussen, 2007; Rose and
175 Koenigswald, 2007). The ischyromyine, *Ischyromys* was also probably fossorial based on
176 postcranial data (Wood, 1937). The Reithroparamyine, *Reithroparamys* was scansorial but may
177 have potentially spent more time in the trees than *Paramys* (Wood, 1962, Rose and Chinnery,
178 2004). No postcrania have been recovered for *Rapamys* and *Titanotheriomys* and it remains
179 unclear if these genera exhibited similar locomotor modes to their close relatives *Reithroparamys*
180 and *Ischyromys* respectively. In contrast, a recent study found that some members of these three
181 subfamilies (i.e. *Paramys*, *Reithroparamys*, *Rapamys* and *Ischyromys*) were terrestrial based on
182 cranial dimensions (Bertrand et al., 2016a). This result may indicate that ischyromyids were
183 more conservative in terms of cranial shape compared to squirrels, which show cranial
184 adaptations based on locomotor mode (Luo et al., 2014). Our Sciuridae sample includes two

185 Oligocene fossils, the Sciurini *Protosciurus* considered arboreal based on postcranial data (Korth
186 and Samuels, 2015), and *Cedromus* for which no postcranial data has been discovered to date.
187 The postcrania of *Prosciurus* have previously been interpreted as squirrel-like, which suggest
188 they it have been arboreal (Hopkins, 2007). The early Miocene *Mesogaulus* displays cranial
189 adaptations for fossoriality, also present in other Mylagaulinae known for being fossorial
190 (Hopkins, 2008).

191 From previous analyses of SCC dimensions (Spoor et al., 2007; Malinzak et al., 2012),
192 we expect rodents with relatively faster locomotor behaviours to have relatively larger and more
193 orthogonal SCCs in comparison to rodents with slower locomotor behaviours. Fossil rodents
194 inferred to have had relatively agile locomotor behaviours (e.g., arboreal behaviour) including
195 early Sciuroidea are expected to have relatively larger SCCs. In contrast, rodents that have been
196 suggested to practice less agile locomotion (i.e., generalist, terrestrial or fossorial behaviours),
197 including the fossorial *Pseudotomus*, and the aplodontid *Mesogaulus*, are expected to have
198 relatively smaller and less orthogonally positioned SCCs. The current sample allows for
199 consideration not only of individual species' locomotor behaviours, but patterns in change
200 through time for the early phases of rodent evolution.

201

202 **Institutional abbreviations**

203 AMNH, American Museum of Natural History, New York, NY; AMNH F:AM, Frick collection:
204 American Museum of Natural History, New York, NY; USNM, United State National Museum,
205 Washington, D.C.; ROMV, Royal Ontario Museum Vertebrate Paleontology; YPM, Yale
206 Peabody Museum, New Haven, CT.

207

208

209 **Materials and Methods**

210 **Materials**

211 High resolution microCT scans were obtained for fossil and extant rodent crania at the
212 Shared Materials Instrumentation Facility (SMIF), Duke University, North Carolina or the
213 Microscopy and Imaging Facilities (MIF) of the American Museum of Natural History, New
214 York (Table S1). Semicircular canal dimensions were measured for twelve fossil rodent crania
215 including eight ischyromyids, two sciurids, and two apodontids (Table 2). The majority of the
216 fossil rodents are from the early Eocene to Oligocene while *Mesogaulus paniensis* is from the
217 early Miocene (Table 2). The fossil sample was chosen based on availability of well-preserved
218 specimens in museum collections. The modern comparative dataset from Spoor and colleagues
219 (2007) includes SCC dimensions for 210 mammals including thirty-eight extant rodents from
220 various families including Anomaluridae, Bathyergidae, Castoridae, Caviidae, Chinchillidae,
221 Dipodidae, Erethizontidae, Hydrochaeridae, Muridae, Myocastoridae, Pedetidae, Sciuridae, and
222 Spalacidae. We measured SCC dimensions for an additional eighteen extant rodents to make the
223 comparative sample more relevant to the fossils under study by expanding the taxonomic and
224 ecological diversity in the sample. These include the only living apodontid, *A. rufa* and
225 seventeen species of Sciuridae (Table 3). We use one specimen for each species except for
226 *Ischyromys typus*, for which two specimens were used (Table 2). Additional information
227 regarding scanning acquisition can be found in Table S1.

228 **Methods**

229 Semicircular canal dimensions were measured from the left inner ear of each specimen
230 unless this side was not sufficiently well preserved. In such cases, measurements were taken
231 from the right inner ear (indicated with an asterisk in Tables 2 and 3). On a WACOM Cintiq
232 21UX tablet, TIFF images of the CT data were visualized in ImageJ (Rasband, 1997-2014) and
233 cropped around the bony labyrinth for each specimen to minimize the overall size of the dataset.
234 Using AVIZO® 7.0.1 software (Visualization and Sciences Group, 1995-2012), the data were re-
235 sliced so that each SCC could be visualized in a single plane following the approach of Spoor et
236 al. (2007; see also Silcox et al., 2009). This was done by visualizing the dataset in orthogonal
237 view using the Slice module and identifying each canal based on characteristic anatomical
238 relationships (Fig. S1). The “fit to point” feature of the Slice module allows 3 points to be placed
239 along the length of each SCC, to orient the slice in the resulting plane (Fig. 2). We measured arc
240 height and width as outlined in Spoor et al. (2007) to calculate the average SCC radius (Fig. 2;
241 Table S1). They are measured as the maximum length from one side to the other, taken from the
242 center of the lumen (Fig. 2). Arc height and width has been previously described by Spoor and
243 Zonneveld (1995) among other standardized measurements of the bony labyrinth in humans and
244 other primates. The anterior SCC radius (ASR), posterior SCC radius (PSR) and lateral SCC
245 radius (LSR) were calculated as follows:

$$246 \quad R = 0.5 \left(\frac{h + w}{2} \right)$$

247 Where R is the radius of each canal (i.e., ASR, PSR, and LSR), h is the height and w is
248 the width. Furthermore, the average radius for all three SCCs (SCR) is calculated from ASR,
249 PSR and LSR.

250 Using video footage and field observations, Spoor et al. (2007) assigned agility scores to
251 extant mammals. Silcox et al. (2009) published regression equations to calculate agility scores
252 for mammals using the Spoor et al. (2007) dataset. Because it may not be possible to recover all
253 three SCCs for a particular specimen, depending on preservation and the quality of the data, they
254 provided separate equations utilizing ASR, PSR, LSR as well as SCR. Here, we present agility
255 scores utilizing the equation for SCR and LSR. The LSR has been found to be the best predictor
256 of agility level (Silcox et al., 2009), likely because the lateral canal is the least constrained by the
257 size and morphology of the petrosal lobule (Jeffery et al., 2008). For this reason, SCC
258 dimensions are primarily analyzed using the LSR.

259 Although we calculate agility scores for the specimens in our sample (Table 3), in light of
260 the qualitative approach used by Spoor et al. (2007) in assigning agility categories, we also
261 examine the data directly through bivariate plots of \log_{10} LSR (logarithm of lateral SCC radius)
262 vs. \log_{10} BM (logarithm of body mass) for our sample with the rodents from Spoor et al. (2007;
263 Table S2), and with the full mammal dataset from Spoor et al. (2007; Table S3). Furthermore, we
264 use residuals from the least squares regression of \log_{10} LSR and \log_{10} BM to analyze variation in
265 relative LSR of our extant and fossil rodents relative to the dataset from Spoor et al. (2007) with
266 extant rodents (Table S2) and all mammals (Table S3). Least squares regression analysis is used
267 to remain consistent with methods from Spoor et al (2007) for analyzing the modern comparative
268 dataset. The Kruskal-Wallis test is used to test for differences in the residuals from \log_{10} LSR and
269 \log_{10} BM between different rodent groups. This non-parametric test allows for the statistical
270 comparison of residuals based on sample medians between multiple groups and is ideal in
271 situations of low sample size, as is the case for most of our groups (Madrigal, 1998). The Dunn's
272 non-parametric post hoc test was used to assess where the significant differences between groups

273 lie. We present p-values with Bonferroni corrections. These tests were performed using PAST
274 3.16 (Hammer et al., 2001) to compare residuals for 1) all mammals from Spoor et al. (2007)
275 grouped by agility with extant rodents as a separate group and 2) fossil rodents grouped by
276 agility.

277 Manual segmentation of the bony labyrinth was also performed in AVIZO® 7.0.1 software
278 (Visualization and Sciences Group, 1995-2012) using the Segmentation Editor (Fig. 3) for each
279 specimen. The segmented bony labyrinth was used to obtain measurements of SCC orthogonality
280 using the same side from which radii of curvature were measured. Following segmentation, an
281 STL ascii surface file was generated and the Autoskeletonization feature in AVIZO was used to
282 generate midline curves for each SCC. The midline curves represent the exact center of the
283 lumen of each SCC. Measurements of orthogonality were obtained by defining the plane of each
284 SCC, composed of 3 points on the midline curve. Angle measurements of the ipsilateral canal
285 pairs were calculated between the resulting planes, including the angle between the anterior SCC
286 and lateral SCC (ASC/LSC angle), posterior SCC and lateral SCC (PSC/LSC angle) and anterior
287 SCC and posterior SCC (ASC/PSC angle; Tables 4, S4). $\text{Log}_{10}\text{AVM}$ (logarithm of the angular
288 velocity magnitude) was calculated for our sample, which provides an estimation of the head's
289 rotational speed, modelled from a modern primate comparative sample (Table 4; see Malinzak et
290 al., 2012). The following formula from Malinzak et al. (2012) was used to calculate $\text{log}_{10}\text{AVM}$:

$$291 \quad \text{Log } 10 (\text{AVM}) = -0.51 \times \text{Log } 10 (90\text{VAR}) + 2.83$$

292 Here, 90VAR is the sum of the angular deviation from 90 degrees for all three SCC pairs. The
293 calculated $\text{log}_{10}\text{AVM}$ and 90 VAR for all rodents were compared to data from Malinzak et al.
294 (2012) including 5 primates and 2 non-primate species, *Cynocephalus volans* and *Bradypus*
295 *variegatus*. [In order to obtain a more accurate idea of how 90VAR covaries with LSR in our](#)

296 fossil and extant rodent sample, $\log_{10}90\text{VAR}$ values were plotted against residuals from the least
297 squares regression of $\log_{10}\text{LSR}$ and $\log_{10}\text{BM}$. Therefore, we were able to analyze 90VAR
298 independently of AVM, which is calculated in part, using 90VAR.

299 Body mass is an important factor in this analysis, as previous work (Spoor et al., 2007)
300 has shown that the strongest factor controlling SCC size is body size, so this variable must be
301 controlled for when seeking a locomotor signal. Skeletal elements from which body mass can be
302 estimated are quite limited for fossil rodents in this study since many are unknown from
303 postcrania. Dental data from extant rodents have often been used to estimate body mass in fossil
304 rodents (e.g., Legendre, 1986; Gagnon, 1996; Martin, 1996; Antoine et al., 2012). However, due
305 to the derived nature of many extant rodent teeth, an accurate body mass estimation from dental
306 measures is difficult to obtain (Bertrand et al., 2016a). Bertrand et al. (2016a) showed that
307 cranial length was a reliable indicator of body mass for many of the fossil rodents in the current
308 study. Therefore, this study utilized cranial length to estimate body mass of fossil rodents. In
309 cases where cranial length was not available, cheek-tooth area was used, which is another
310 reliable estimator of body mass (Bertrand et al., 2016a; Table S1).

311

312 **Results**

313 **Radii of curvature of the semicircular canals**

314 The relationship between body mass and LSC radius for the eighteen extant rodents
315 measured in this study is shown in the broader context of the data for rodents from Spoor et al.
316 (2007) in Figure 4 and for all mammals from Spoor et al. (2007) in Figure 5. Modern sciurids
317 have large LSCs relative to body mass, plotting among the fast-moving rodents (Fig. 4) and fast-

318 moving mammals in general (Fig. 5). This result is consistent with expectations from their
319 behavioural data, since they are mostly active arboreal/scansorial animals, with a few (i.e.,
320 *Rhinosciurus*, *Lariscus*) being terrestrial, but still fairly agile. As a result, this group has some of
321 the highest residuals calculated from the least squares regression between $\log_{10}\text{LSR}$ and $\log_{10}\text{BM}$
322 and fall in the range of fast moving rodents (Fig. 4B) and fast moving mammals (Fig. 5B) from
323 Spoor et al. (2007).

324 The Kruskal-Wallis test shows that a significant difference exists among the 6
325 mammalian agility groups and extant sciurids in terms of median residuals [$H(\chi^2) = 52.59$; $p =$
326 1.42×10^{-9} ; Table 5]. The Dunn's post hoc test supports previous inferences (Spoor et al., 2007)
327 that there are significant differences in relative SCC canal sizes among most of the agility
328 groupings, with a few exceptions (Table 5). This test also shows that the median residuals of
329 extant sciurids differ significantly from mammalian groups categorized as extremely slow, slow,
330 medium slow, and medium (Table 5). The median of extant sciurids does not differ from the
331 medians of the mammalian groups categorized as medium fast and fast (Table 5). On the other
332 hand, *Aplodontia* has a relatively smaller LSC for its body mass, falling among the slowest
333 modern rodents from Spoor et al. (2007; Fig. 4A) with a residual value that is much lower than
334 modern squirrels and is in the range of relatively slower rodents from Spoor et al (2007; Fig.
335 4B). The agility score for *Aplodontia* is 4.0 (medium) based on LSR and 2.9 (medium-slow)
336 based on SCR (Table 3).

337 The included fossil rodents have smaller LSCs relative to body mass (Fig. 4A), with
338 residuals for this group calculated from $\log_{10}\text{BM}$ and $\log_{10}\text{LSR}$ being well below zero (Fig. 4B).
339 They group with modern rodents from Spoor et al. (2007) categorized as medium to slow. In
340 contrast, Reithroparamyinae (*Reithroparamys* and *Rapamys*) have relatively larger LSCs,

341 grouping among rodents categorized by Spoor et al. (2007) as having fast and medium agility
342 (Fig. 4). Members of Ischyromyinae, however, show considerable variability in their agility
343 scores (Table 6). The ischyromyine *Titanotheriomys* has a relatively larger LSC compared to
344 *Ischyromys* and groups with rodents categorized by Spoor et al. (2007) as having fast and
345 medium agility (Fig. 4). In contrast, *Ischyromys* groups with rodents categorized by Spoor et al.
346 (2007) as slow and medium (Fig. 4). Hence, the residuals for *Reithroparamys*, *Rapamys* and
347 *Titanotheriomys* are found to be greater than those calculated for *Paramys*, *Pseudotomus* and
348 *Ischyromys* (Fig. 4).

349 Both fossil squirrels, *Cedromus* and *Prosciurus* have large SCCs relative to body mass,
350 in the range of extant sciurids, resulting in much higher calculated residuals (Fig. 4). Both taxa
351 group with rodents categorized by Spoor et al. (2007) as having fast locomotion (Fig. 4). In
352 contrast, the two members of Aplodontidae vary considerably in LSC radius, with the early
353 Oligocene *Prosciurus* having a larger LSC (and higher residual) compared to the early Miocene
354 *Mesogaulus*, which has a much lower residual, close to the ischyromyids *Paramys* and
355 *Ischyromys* (Fig. 4). *Prosciurus* groups with rodents from Spoor et al. (2007) categorized as
356 having fast locomotion, while *Mesogaulus* is close to *Aplodontia* and rodents with relatively
357 slower locomotion (Fig. 4).

358 The agility scores calculated using the all mammal predictive equations from Silcox et al.
359 (2009) are presented in Table 6 for the LSR and average SCR, and these taxa are included in the
360 bivariate plot of $\log_{10}\text{LSR}$ vs. $\log_{10}\text{BM}$ in Figure 5. The pattern of variation is similar to that
361 described for the rodent sample, with notable variation in the residuals calculated from the least
362 squares regression line among the fossil taxa. Indeed, these residuals can be used to divide the
363 fossil rodent sample into three groups, which coincide with the ranges of their respective agility

364 scores (Fig. 6): 1) rodents with low residuals (median = -0.041) and medium slow to medium
365 agility scores (*Paramys*, *Ischyromys*, and *Mesogaulus*); 2) rodents with intermediate residuals
366 (median = 0.028) and medium to medium fast agility scores (*Reithroparamys*, *Rapamys*, and
367 *Titanotheriomys*); and 3) rodents with high residuals (median = 0.097) and medium fast to fast
368 agility scores (*Cedromus*, *Protosciurus*, and *Prosciurus*). A Kruskal Wallis test shows that there
369 is a significant difference between the 3 groups and median residuals ($p=0.0093$). A Dunn's post
370 hoc test reveals a significant difference between the groups with the highest and lowest residuals
371 ($p=0.0033$). However, the median residuals for the intermediate fossil rodent group is not
372 significantly different from the other two groups (Fig. 6).

373

374 **Semicircular canal orthogonality**

375 Measurements of the angles between the SCCs are shown in Tables 4 and S4. Extant
376 rodents have the greatest variation in 90 VAR for the ASC/LSC pair (variance = 17.7) compared
377 to the ASC/PSC pair (variance = 7.1) and PSC/LSC pair (variance = 8.7; Table S4). This is
378 consistent with previous findings from living and fossil primates where 90 VAR for the
379 ASC/LSC angle showed the greatest variation (Malinzak et al. 2012; Berlin et al. 2013; Bernardi
380 and Couette, 2017). In contrast, variation in 90 VAR for fossil rodents only differs slightly
381 between the three canal pairs: ASC/LSC pair (variance = 8.6), ASC/PSC pair (variance = 8.5)
382 and PSC/LSC pair (variance = 9.0; Table S4).

383 The angular velocity magnitude quantifies the rotational speed of the head. The average
384 \log_{10} AVM value calculated for extant sciurids is 2.25 ± 0.11 with values ranging from 2.1 to 2.45
385 (Table 4). The average \log_{10} AVM value for fossil rodents is 2.26 ± 0.09 with values ranging from

386 2.11 to 2.43 (Table 4). All rodents have high \log_{10} AVM values and relatively low \log_{10} 90VAR
387 and group towards the top left of the distribution with the fastest moving primates from Malinzak
388 et al. (2012; Fig. 7A). This result implies that rodent SCCs are relatively more orthogonal
389 compared to slower moving primates. Rodent \log_{10} AVM values encompass and extend beyond
390 the range of two of the fastest primates from Malinzak et al (2012): 1) the leaper *Galago moholi*
391 with the highest \log_{10} AVM value for all primates and 2) the arboreal quadrupedal *Cheirogaleus*
392 *medius*, with the second highest \log_{10} AVM value (Fig. 7A). Consistent with results from
393 Malinzak et al. (2012), the \log_{10} AVM for the glider *Cynocephalus* (colugo) remains the highest
394 calculated, while *Bradypus* (brown-throated sloth) remains the lowest (Fig. 7A). However, no
395 discernible trends are apparent in the \log_{10} AVM distribution for rodents. For example, the fast
396 moving extant sciurids, that would be expected to have relatively more orthogonal SCCs, are
397 found widely distributed along the \log_{10} AVM and \log_{10} 90VAR scales (Fig. 7A). Furthermore,
398 the slow-moving *Aplodontia* would be expected to have a relatively low \log_{10} AVM, however, it
399 plots much higher up, among fast moving sciurids. Fossil taxa fall within the range of variation
400 of the extant sciurids, with the fastest moving non-rodent taxa. Ischyromyines might have been
401 expected to have less orthogonal SCCs, but fall near both the top and bottom of the fossil rodent
402 distribution, with both *Ischyromys* specimens showing the greatest difference (Fig. 7A).

403 Similarly, no discernible trends are found in \log_{10} 90VAR for fossil and extant rodents when
404 compared to residuals from LSR (slope = 0.085, intercept = -0.056, $R^2 = 0.075$; Fig. 7B). Fossil
405 rodents that were found to have low residuals and medium slow to medium agility scores
406 (*Paramys*, *Ischyromys*, and *Mesogaulus*) remain on the lower end of the residual distribution, but
407 are quite spread apart with respect to the \log_{10} 90VAR scale (Fig. 7B).

408

409 Discussion

410 Semicircular canal radii of curvature dimensions and early rodent evolution

411 Ischyromyids are considered to be some of the most primitive rodents, with members of
412 that group likely being ancestral to members of later occurring families such as Sciuridae and
413 Aplodontidae (Korth, 1994). Based on postcranial data, *Paramys* has been reconstructed as being
414 scansorial (Rose and Chinnery, 2004) compared to *Pseudotomus* (Dunn and Rasmussen, 2007)
415 and *Ischyromys* (Wood, 1937), which both displayed more terrestrial to burrowing adaptations.
416 Our results do not seem to match the differences observed in the postcrania of *Paramys* and
417 *Ischyromys* as they both fall in the medium slow to medium locomotor category and had very
418 similar agility scores. However, *Pseudotomus* had the lowest agility score of all ischyromyids,
419 which is in accordance with postcranial data. In light of these results, *Ischyromys* may have been
420 less specialized than *Pseudotomus*. However, it is possible that this discrepancy in agility for a
421 similar style of locomotion could relate to body mass differences, with *Ischyromys* being much
422 smaller than *Pseudotomus*. Additionally, if *Ischyromys* came from a reithroparamyine type
423 ancestor that was more scansorial than *Paramys*, then a higher degree of agility than
424 *Pseudotomus* could have been preserved in this taxon. The agility scores and residuals for
425 members of Reithroparamyinae suggest they had medium to medium fast locomotion. This is
426 consistent with previous inferences that *Reithroparamys* was squirrel-like based on the anatomy
427 of its foot (Wood, 1962) and may suggest that this taxon may have spent more time in trees, or at
428 least was more active than *Paramys*. The inferred more agile locomotion of reithroparamyines
429 compared to paramyines and *Ischyromys* is consistent with the idea that they were moving in the
430 direction of squirrel-like locomotion, and is also consistent with their inferred phylogenetic
431 position as being closely related to the squirrel-related clade (Meng, 1990).

432 These categorizations are consistent with the residuals calculated from the least squares
433 regression of \log_{10} LSR and \log_{10} BM where *Paramys*, *Pseudotomus* and *Ischyromys* have smaller
434 residuals compared to the reithroparamines and *Titanotheriomys*, which are relatively higher
435 (Fig. 6). However, the Dunn's post hoc test did not reveal a significant difference between the
436 median residuals of these groups, which may be attributed to the low sample size (Fig. 6).
437 Despite this fact, the groupings based on residuals as well as the reconstructed agility scores
438 provide some insight on the locomotor mode of ischyromyids. The Oligocene *Ischyromys* has
439 some of the lowest agility scores (3.8 and 4 for LSR) and fall in the smallest residual group (Fig.
440 6) while, taxa such as *Reithroparamys* and *Rapamys* have relatively higher scores (4.4 and 4.6
441 respectively for LSR) and fall in the intermediate residual group (Fig. 6).

442 The ancestor of Ischyromyidae was probably scansorial based on our results and on the
443 inference that the most basal ischyromyid of our sample, *Paramys*, exhibited this behaviour.
444 During the Eocene, *Pseudotomus* invaded a new type of ecological niche and become more
445 fossorial, while other ischyromyids (i.e., *Reithroparamys*, *Rapamys* and *Titanotheriomys*)
446 followed a different trajectory by becoming more agile, and were probably spending more time
447 in trees as a result. During the Oligocene, *Ischyromys* became more fossorial departing from a
448 hypothetical reithroparamyine scansorial ancestor, converging with the Eocene *Pseudotomus* in
449 terms of locomotor behavior. Ultimately, ischyromyid agility reconstructions are in agreement
450 with the idea that this group displayed a variety of locomotor modes. Those that were not
451 exclusively arboreal, such as generalist, terrestrial or fossorial rodents, were found to have
452 relatively smaller LSCs, while those with greater adaptations for arboreality were found to have
453 relatively larger LSCs.

454

455 **Locomotor behavior in Sciuroidea**

456 Making inferences regarding the locomotor behaviour of early sciurids is difficult as
457 many specimens are unknown from postcranial material. Evidence from early fossil sciurids
458 suggests that they were likely arboreal and that this locomotor behaviour was an ancestral trait
459 for this group (Emry and Thorington, 1982). However, *Cedromus* is unknown from postcranial
460 material and is placed outside of extant squirrels. Aspects of *Cedromus* endocranial anatomy
461 (e.g., caudal expansion of the neocortex, large petrosal lobules) have led Bertrand et al. (2017) to
462 interpret these features as indicative of improved vision, which may be consistent with arboreal
463 locomotion. *Cedromus* has a LSR in the range of fast moving rodents such as the tree squirrel
464 *Sciurus* (Fig. 5A). The fact that *Cedromus* falls in the highest residual group (Fig. 6) and has a
465 high agility score in the fast agility range is consistent with an active and arboreal locomotor
466 behaviour.

467 *Aplodontia* predominantly displays fossorial locomotor behaviour (Carraway and Verts,
468 1993) and its low agility score inferred from its relatively small LSC (Figs. 4 and 5), reflects the
469 fact that fossorial animals are likely to experience smaller degrees of angular accelerations of the
470 head than animals that are actively locomoting through the trees or hopping on the ground. As
471 such, this result is more consistent with expectations from behaviour than the results for fossorial
472 rodents in Pfaff (2015). In contrast, early aplodontids show squirrel-like adaptations, suggesting
473 they had arboreal and scansorial locomotor behaviours (Hopkins, 2005; 2008). The early
474 aplodontid *Prosciurus* has a relatively larger LSC and groups with fast moving taxa such as the
475 flying squirrel *Glaucomys* (Fig. 5A) and falls in the high residual group (Fig. 6). Furthermore,
476 *Prosciurus* yielded the highest agility score (6.1 from the LSC) out of all fossil rodents and can
477 be reconstructed as having fast, agile locomotor behaviour. This is in line with previous

478 interpretations of its postcrania by Hopkins (2007), who found that it had squirrel-like
479 adaptations and may have been arboreal. Furthermore, Bertrand et al. (2018) found similarities in
480 the endocranial anatomy (i.e., expanded neocortex, and petrosal lobules) in *Prosciurus*, which
481 resembled arboreal squirrels. The high agility reconstructed for early Oligocene members of both
482 Sciuridae and Aplodontidae is consistent with the inference that arboreality was likely an
483 ancestral trait for Sciuroidea. This group was more adapted to arboreal lifestyle and were more
484 agile than their ischyromyid ancestors.

485 More derived members of Sciuroidea in our sample include the late Oligocene sciurid
486 *Protosciurus* and the early Miocene aplodontid *Mesogaulus*. *Protosciurus* is known from
487 postcrania and has been considered arboreal (Korth and Samuels, 2015). Its high agility score
488 and placement in the high residual group (Fig. 6) is consistent with this behavioural
489 reconstruction. This finding suggests that this taxon had fast, agile locomotion comparable to
490 extant tree squirrels (Fig. 5A). On the other hand, *Mesogaulus* has a relatively lower agility score
491 (Table 6) and falls in the low residual group (Fig. 6). This suggests that this species displayed
492 medium slow to medium locomotion, similar *Aplodontia* and some ischyromyids (i.e., *Paramys*
493 and *Ischyromys*). *Mesogaulus* also has relatively smaller SCCs compared to *Prosciurus* (Figs. 4
494 and 5), which is consistent with its postcranial reconstruction indicating that it was a specialized
495 burrower (Hopkins, 2008). *Mesogaulus* and *Aplodontia* can be inferred to have had similar
496 locomotor adaptations, because of their relatively similar LSC sizes (Figs. 4 and 5) and agility
497 scores. The relatively slower locomotor reconstruction of *Mesogaulus* is in line with inferences
498 that derived aplodontids became more fossorial through time compared to their arboreal
499 ancestors (Hopkins, 2007). Bertrand et al. (2018) found that *Mesogaulus* had a smaller neocortex

500 and petrosal lobules, which might indicate that this taxon was spending more time underground
501 and required less vision to survive.

502

503 **Semicircular canal orthogonality and rodent locomotor behaviour**

504

505 The second method used, which analyzes the angles between the SCCs, relies on the
506 relationship between SCC orthogonality (90VAR) and angular velocity magnitude (AVM).
507 Animals with more orthogonal SCCs (lower 90VAR) are expected to have greater angular head
508 velocities compared to animals with less orthogonal SCCs (higher 90VAR). Semicircular canal
509 orthogonality is used to calculate angular velocity magnitude (AVM) based on the primate
510 dataset and equation from Malinzak et al. (2012). The \log_{10} AVM values for primates range from
511 1.82 for slow moving species and 2.36 for fast moving species. Rodents have \log_{10} AVM values
512 and SCCs that are generally more orthogonal (lower \log_{10} 90VAR values) than primates, however
513 there is some overlap with the two most agile primates (Fig. 7A). Within the rodent sample,
514 \log_{10} AVM scores did not follow patterns of locomotor behaviour. For example, the extant
515 sciurids, who exhibit agile, arboreal locomotion, were found widely distributed along the
516 \log_{10} AVM and \log_{10} 90VAR scales (Fig. 7A). Additionally, *Aplodontia rufa* was found to have a
517 much higher \log_{10} AVM value and more orthogonal SCCs (Fig. 7A) than would be expected
518 based on its less agile, fossorial adaptations. These results suggest that the comparative dataset
519 from Malinzak et al. (2012) may not be applicable to non-primate groups such as rodents. This is
520 further exemplified in the comparison of \log_{10} 90VAR and residuals from LSR, which has a
521 relatively weak R^2 value of 0.075. The applicability of this method to primate groups beyond
522 strepsirrhines has also been questioned and a recent study showed an unexpectedly broad range

523 of \log_{10} AVM values for multiple specimens of the fossil primate *Adapis parisiensis*, which
524 ranged the entire primate \log_{10} AVM scale (Bernardi and Couette, 2017).

525 The fact that this method does not factor in any element of body size may be one reason
526 for the broad range of \log_{10} AVM scores. A recent study analyzing intraspecific variation in
527 primates using SCC dimensions (i.e., radii of curvature and canal angles), demonstrates the
528 importance of body size in such analyses. For both strepsirrhine and platyrrhine primate groups,
529 functional differences in SCC morphology, driven partly by variation in orthogonality, were only
530 distinguishable when body size was accounted for (Gonzales et al., 2018). Another reason for the
531 broad range of \log_{10} AVM scores may have to do with the way SCC shape varies based on
532 function between taxa. Gonzales et al. (2018) highlighted the idea that vertebrates may employ
533 more than one morphological strategy in detecting the environment through angular head
534 rotations. In fact, divergent adaptations of the vestibular system have been documented in
535 fossorial ceacilians (Maddin and Sherratt, 2014) and snakes (Yi and Norell, 2015). In this
536 respect, rodents may have developed a different SCC shape based on function, which relies less
537 on orthogonality and more on SCC size compared to other groups.

538

539 **Limitations to using SCC radii of curvature dimensions**

540 Limitations exist when using the Spoor et al. (2007) method with respect to the agility
541 scores that are calculated. Since the designation of agility level in the modern comparative
542 dataset was performed in a qualitative manner (Spoor et al., 2007), it is fair to raise questions
543 regarding the information content of the reconstructed agility scores for fossil rodents. Also, in
544 modern mammals, considerable overlap exists between different agility categories (Fig. 5). For

545 example, in terms of the relative size of the LSR, some mammals in the fast category are found
546 to range as low as mammals in the slow category, while mammals grouped in the medium
547 category vary extensively, with their range covering mammals categorized as slow, medium
548 slow, medium, medium fast and fast (Fig. 5). Unfortunately, besides the dataset from Malinzak
549 et al. (2012) which uses direct measurements of angular head velocity, no other comparative
550 datasets exist that have assessed agility in a more quantitative methodology. The Spoor et al.
551 (2007) dataset remains the largest and most diverse sample for which an agility assessment is
552 available. Within the context of the current analysis, the results from the SCC radii data
553 (considered using either residuals or agility scores) are consistent with the locomotor data that
554 are available for some of the taxa in the sample, and in fact seem to tell a compelling story of
555 increasing agility with adaptations for arboreality in some lineages, and decreasing agility in
556 groups that become more fossorial. In contrast, the data from the orthogonality analysis do not
557 seem to show any clear relationship to previously inferred patterns of locomotor behaviour.

558

559 **Conclusions**

560 The SCCs serve as an independent source of data to infer locomotor behaviour of fossil
561 species that are unknown from postcranial material. This study is the first to use SCC dimensions
562 to reconstruct locomotor agility for fossil rodents. The variability in relative LSC size and agility
563 scores among Ischyromyidae supports previous interpretations that they had diverse locomotor
564 behaviours (e.g., Wood, 1937; Rose and Chinnery, 2004; Dunn and Rasmussen, 2007;). Some
565 taxa such as *Paramys*, *Pseudotomus* and *Ischyromys* had relatively lower inferred agility
566 compared to the faster moving reithroparamyines. The fast locomotor agility reconstructions for

567 early sciuroids, suggests they were fast and highly agile animals and supports previous findings
568 suggesting that the common ancestor for this group was most likely arboreal (Emry and
569 Thorington, 1982; Hopkins, 2005; 2008). The low agility of *Ischyromys* might be a derived
570 condition, while the higher agility exhibited in *Reithroparamys* might show a transition from
571 scansorial ischyromyid to highly arboreal early sciuroids. In later aplodontids, a decrease in
572 inferred agility level is observed, which is consistent with previous work suggesting that these
573 later members displayed terrestrial to fossorial adaptations (Hopkins, 2008).

574 All considered, fossil rodent agility reconstructions speak to our understanding of major
575 evolutionary transitions in rodents. Viewed from another perspective, the impressive consistency
576 between the inferences previously made based on postcranial and endocranial data for shifts in
577 locomotor type in rodent evolution, and the patterns in SCC size observed here, serve to validate
578 the value of these dimensions to understanding broad-scale patterns of locomotor evolution
579 through time. In contrast, the lack of such agreement with calculated orthogonality measures
580 suggests that variation in this parameter is not informative with respect to locomotor behaviour
581 in rodents.

582

583 **Acknowledgements**

584 The authors would like to thank D. Bohaska, and N.D. Pyenson from the Paleontology
585 Department of the Smithsonian (NMNH), J. Meng, R. O'Leary and E. Westwig from the
586 American Museum of Natural History (AMNH) as well as D. Brinkman, M. Fox and Chris
587 Norris from the Yale Peabody Museum for providing access to the specimen to be scanned. The
588 authors also thank J. Thostenson and D.M. Boyer for facilitating the scanning of the specimens at

589 the SMIF (Duke University) and M. Hill from the AMNH Microscopy and Imaging Facility for
590 scanning the specimens. This research was supported by an NSERC Discovery Grant to MTS
591 and Marie Skłodowska-Curie Actions: Individual Fellowship (H2020-MSCA-IF-2018-2020; No.
592 792611) to OCB. The very constructive comments from Philip Cox and one anonymous reviewer
593 considerably strengthened this paper. This project is dedicated to the memory of the great
594 scholar, valued mentor and good friend Alan C. Walker (1938-2017), who started one of us
595 (MTS) on the study of semicircular canals almost 20 years ago.

596

597 **Author Contributions**

598 RB, OCB and MTS all contributed to the conception and design of the study and the analysis and
599 interpretation of the data. For each specimen, OCB acquired the CT data, RB collected
600 measurements and reconstructed agility. RB drafted the article and OCB and MTS revised it
601 critically. All authors gave final approval before submission.

602

603 **Data Availability Statement**

604 The surface renderings of the bony labyrinth endocasts described in this paper are available on
605 MorphoSource (www.morphosource.org; Boyer et al. 2014) at
606 https://www.morphosource.org/MyProjects/Dashboard/dashboard/select_project_id/1030

607

608 **References**

609 **Anderson, D** (2008) Ischyromyidae. In: *Evolution of Tertiary Mammals of North America*. (eds
610 Janis CM, Gunnell GF, Uhen MD) pp 311-325. Cambridge: Cambridge University Press.

- 611 **Antoine P-O, Marivaux L, Croft DA, et al.** (2012) Middle Eocene rodents from Peruvian
612 Amazonia reveal the pattern and timing of caviomorph origins and biogeography. *Proc R*
613 *Soc B* **279**, 1319–1326.
- 614 **Asher RJ, Smith MR, Rankin A, et al.** (2019) Congruence, fossils and the evolutionary tree of
615 rodents and lagomorphs. *R Soc Open Sci* **6**, 190387.
- 616 **Berlin JC, Kirk EC, Rowe TB** (2013) Functional implications of ubiquitous semicircular canal
617 non-orthogonality in mammals. *PLoS ONE* **8**, e79585.
- 618 **Bernardi M, Couette S** (2017) Eocene paleoecology of *Adapis parisiensis* (Primate, Adapidae):
619 from inner ear to lifestyle. *Anat Rec* **300**, 1576-1588.
- 620 **Bertrand OC, Silcox MT** (2016) First virtual endocasts of a fossil rodent: *Ischyromys typus*
621 (Ischyromyidae) and brain evolution in rodents. *J Vertebr Paleontol* **36**, 1–19.
- 622 **Bertrand OC, Schillaci MA, Silcox MT** (2016a) Cranial dimensions as estimators of body
623 mass and locomotor habits in extant and fossil rodents. *J Vert Paleontol* **36**, 1–10.
- 624 **Bertrand OC, Amador-Mughal F, Silcox MT** (2017) Virtual endocast of the early Oligocene
625 *Cedromus wilsoni* (Cedromurinae) and brain evolution in squirrels. *J Anat* **230**, 128-151.
- 626 **Bertrand OC, Amador-Mughal F, Lang MM, Silcox MT** (2018) Virtual endocasts of fossil
627 Sciuroidea: brain size reduction in the evolution of fossoriality. *Palaeontology* **61**, 919–
628 948.
- 629 **Bertrand OC, Shelley SL, Wible JR, et al.** (2020) Virtual endocranial and inner ear endocasts
630 of the Paleocene ‘condylarth’ *Chriacus*: New insight into the neurosensory system and
631 evolution of early placental mammals. *J Anat* **236**, 21-49.

- 632 **Billet G, Hautier L, Lebrun R** (2015) Morphological diversity of the bony labyrinth (inner ear)
633 in extant xenarthrans and its relation to phylogeny. *J Mammal* **96**, 658-672.
- 634 **Blanga-Kanfi S, Miranda H, Penn O, et al.** (2009) Rodent phylogeny revised: analysis of six
635 nuclear genes from all major rodent clades. *BMC Evol Biol* **9**, 71.
- 636 **Boyer DM, Kaufman S, Gunnell GF, et al.** (2014) Managing 3D digital data sets of
637 morphology: MorphoSource is a new project-based data archiving and distribution tool.
638 *Am J Phys Anthropol* **153**(Suppl 58), 84.
- 639 **Burgin CJ, Colella JP, Kahn PL, et al.** (2018) How many species of mammals are there?. *J*
640 *Mammal* **99**, 1-14.
- 641 **Cameron J, Shelley SL, Williamson TE, et al.** (2019) The brain and inner ear of the early
642 Paleocene “Condylarth” *Carsiptychus coarctatus*: implications for early placental
643 mammal neurosensory biology and behavior. *Anat Rec* **302**, 306–324.
- 644 **Carraway LN, Verts BJ** (1993) *Aplodontia rufa*. *Mammalian Species* **431**, 1-10.
- 645 **Charles-Dominique P** (1977) *Ecology and Behaviour of Nocturnal Primates*. New York:
646 Columbia University Press.
- 647 **Churakov G, Sadasivuni MK, Rosenbloom KR, et al.** (2010) Rodent evolution: back to the
648 root. *Mol Biol Evol* **276**, 1315–1326.
- 649 **Cox PG, Jeffery N** (2010) Semicircular canals and agility: The influence of size and shape
650 measures. *J Anat* **216**, 37-47.

- 651 **Dunn RH, Rasmussen DT** (2007) Skeletal morphology and locomotor behavior of
652 *Pseudotomus eugenei* (Rodentia, Paramyinae) from the Uinta Formation, Utah. *J Vert*
653 *Paleontol* **27**, 987-1006.
- 654 **Emry RJ, Thorington Jr RW** (1982) Descriptive and comparative osteology of the oldest fossil
655 squirrel, *Protosciurus* (Rodentia: Sciuridae). *Smithson Contrib Paleobiol* **47**, 1–35.
- 656 **Fabre PH, Hautier L, Dimitrov D, et al.** (2012) A glimpse on the pattern of rodent
657 diversification: a phylogenetic approach. *BMC Evol Biol* **12**, 1–19.
- 658 **Flynn LJ, Jacobs LL** (2008) Aplodontoidea. In: *Evolution of Tertiary Mammals of North*
659 *America*. (eds Janis CM, Gunnell GF, Uhen MD) pp 377– 390. Cambridge: Cambridge
660 University Press.
- 661 **Gagnon M** (1996) Ecological diversity and community ecology in the Fayum sequence (Egypt).
662 *J Hum Evol* **32**, 133–160.
- 663 **Gebo DL** (1987) Locomotor diversity in prosimian primates. *Am J Primatol* **13**, 271-281.
- 664 **Gonzales LA, Malinzak MD, Kay RF** (2018) Intraspecific variation in semicircular canal
665 morphology – A missing element in adaptive scenarios? *Am J Phys Anthropol* **168**, 10–
666 24.
- 667 **Grohé C, Tseng ZJ, Lebrun R, et al.** (2016) Bony labyrinth shape variation in extant
668 Carnivora: a case study of Musteloidea. *J Anat* **228**, 366–383.
- 669 **Gunz P, Ramsier M, Kuhrig M, et al.** (2012) The mammalian bony labyrinth reconsidered,
670 introducing a comprehensive geometric morphometric approach. *J Anat* **220**, 529–543.

- 671 **Hammer Ø**, Harper DAT, Ryan, P.D. (2001) PAST: Paleontological statistics software package
672 for education and data analysis. *Palaeontologia Electronica* **4**, 9pp.
- 673 **Hopkins SSB** (2005) The evolution of fossoriality and the adaptive role of horns in the
674 Mylagaulidae (Mammalia: Rodentia). *Proc R Soc B* **272**, 1705–13.
- 675 **Hopkins SSB** (2007) Causes of lineage decline in the Aplodontidae: testing for the influence of
676 physical and biological change. *Palaeogeogr Palaeocl* **246**, 331–53.
- 677 **Hopkins SSB** (2008) Phylogeny and evolutionary history of the Aplodontioidea (Mammalia:
678 Rodentia). *Zool J Linn Soc* **153**, 769–838.
- 679 **Hullar TE** (2006) Semicircular canal geometry, afferent sensitivity, and animal behavior. *Anat*
680 *Rec Part A* **288A**, 466–472.
- 681 **Ingles LG** (1960) Tree Climbing by Mountain Beavers. *J Mammal* **41**, 120-121.
- 682 **Jeffery N, Ryan TM, Spoor F** (2008) The primate subarcuate fossa and its relationship
683 to the semicircular canals part II: adult interspecific variation. *J Hum Evol* **55**, 326-339.
- 684 **Koprowski JL, Goldstein EA, Bennett KR, et al.** (2016) Family Sciuridae (tree, flying and
685 ground squirrels, chipmunks, marmots and prairie dogs) In: *Handbook of mammals of the*
686 *world*, volume 6 (eds Wilson DE, Lacher Jr TE, Mittermeier RA) pp 648-837.
- 687 **Korth WW** (1994) *The Tertiary Record of Rodents in North America*. New York: Plenum.
- 688 **Korth WW, Samuels JX** (2015) New rodent material from the John Day Formation (Arikareean
689 and Hemingfordian, middle Oligocene to early Miocene) of Oregon. *Ann Carnegie Mus*
690 **83**, 19–84.

- 691 **Krubitzer L, Campi KL, Cooke DF** (2011) All rodents are not the same: a modern synthesis of
692 cortical organization. *Brain Behav Evol* **78**, 51–93.
- 693 **Lebrun R, Ponce de Leon MS, Tafforeau P, et al.** (2010) Deep evolutionary roots of the
694 strepsirrhine primate labyrinthine morphology. *J Anat* **216**, 368–380.
- 695 **Legendre S** (1986) Analysis of mammalian communities from the late Eocene and Oligocene of
696 southern France. *Palaeovertebrata* **16**, 191–212.
- 697 **Lewis ER, Ellen LL, William SB** (1985) *The vertebrate inner ear*. Boca Raton: CRC Press.
- 698 **Maddin HC, Sherratt E** (2014) Influence of fossoriality on inner ear morphology: Insights from
699 caecilian amphibians. *J Anat* **225**, 83–93.
- 700 **Madrigal L** (1998) *Statistics for anthropology*. Cambridge: Cambridge University Press.
- 701 **Malinzak MD, Kay RF, Hullar TE** (2012) Locomotor head movements and semicircular canal
702 morphology in primates. *Proc Natl Acad Sci USA* **109**, 17914–17919.
- 703 **Marivaux L, Vianey-Liaud MO, Jaeger JJ** (2004) High-level phylogeny of early Tertiary
704 rodents: Dental evidence. *Zool J Linn Soc* **142**, 105–34.
- 705 **Martin RA** (1996) Tracking mammal body size distributions in the fossil record: a preliminary
706 test of the ‘rule of limiting similarity’. *Acta Zool Cracov* **39**, 321–328.
- 707 **Meng J** (1990) The auditory region of *Reithroparamys delicatissimus* (Mammalia, Rodentia)
708 and its systematic implications. *Am Mus Novit* **2972**, 1–35.
- 709 **Meng J, Hu Y, Li C** (2003) The osteology of *Rhombomylus* (Mammalia, Glires): implications
710 for phylogeny and evolution of Glires. *Bull Am Mus Nat Hist* **275**, 1–247.

- 711 **Mennecart B, Costeur L** (2016) Shape variation and ontogeny of the ruminant bonylabyrinth,
712 an example in Tragulidae. *J Anat* **229**, 422-435.
- 713 **Mercer JM, Roth VL** (2003) The effects of Cenozoic global change on squirrel phylogeny.
714 *Science* **299**, 1568–1572.
- 715 **O'Leary MA, Bloch JI, Flynn JJ, et al.** (2013) The placental mammal ancestor and the post-K-
716 Pg radiation of placentals. *Science* **339**, 662-7.
- 717 **Orliac MJ, Gilissen E** (2012) Virtual endocranial cast of earliest Eocene *Diacodexis*
718 (Artiodactyla, Mammalia) and morphological diversity of early artiodactyl brains. *Proc R*
719 *Soc B* **279**, 3670–3677.
- 720 **Pfaff C, Martin T, Ruf I** (2015) Bony labyrinth morphometry indicates locomotor adaptations
721 in the squirrel-related clade (Rodentia, Mammalia). *Proc R Soc B* **282**, 20150744.
- 722 **Rasband WS** (1997–2014) ImageJ. U. S. National Institutes of Health, Bethesda, Maryland.
723 Available at <http://imagej.nih.gov/ij/>. Accessed January 13, 2013.
- 724 **Rose KD, Chinnery BJ** (2004) The postcranial skeleton of early Eocene rodents. *Bull Carnegie*
725 *Mus Nat Hist* **36**, 211–244.
- 726 **Rose KD, Von Koenigswald W** (2007) The marmot-sized paramyid rodent *Notoparamys*
727 *costilloi* from the Early Eocene of Wyoming, with comments on dental variation and
728 occlusion in paramyids. *Bull Carnegie Mus Nat Hist* **39**, 111–25.
- 729 **Ruf I, Volpato V, Rose KD** (2016) Digital reconstruction of the inner ear of *Leptictidium*
730 *auderiense* (Leptictida, Mammalia) and North American leptictids reveals new insight
731 into leptictidan locomotor agility. *Paläontologische Zeitschrift* **90**, 153-171.

- 732 **Ryan TM, Silcox MT, Walker A, et al.** (2012) Evolution of locomotion in Anthroidea: the
733 semicircular canal evidence. *Proc R Soc Lond B* **279**, 3467-3475.
- 734 **Schutz H, Jamniczky HA, Hallgrímsson B, et al.** (2014) Shape-shift: semicircular canal
735 morphology responds to selective breeding for increased locomotor activity. *Evolution*
736 **68**, 3184–3198.
- 737 **Silcox MT, Bloch JI, Boyer DM** (2009) Semicircular canal system in early primates. *J Hum*
738 *Evol* **56**, 315-327.
- 739 **Spoor F, Zonneveld F** (1995) Morphometry of the primate bony labyrinth: a new method based
740 on high-resolution computed tomography. *J Anat* **186**, 271-286.
- 741 **Spoor F, Zonneveld F** (1998) Comparative review of the human bony labyrinth. *Am J Phys*
742 *Anthropol* **27**, 211-251.
- 743 **Spoor F, Garland T, Krovitz G, et al.** (2007) The primate semicircular canal system and
744 locomotion. *Proc Natl Acad Sci USA* **104**, 10808-10812.
- 745 **Thorington RW, Koprowski JL, Steele MA, et al.** (2012) *Squirrels of the world*. Baltimore:
746 JHU Press.
- 747 **Visualization Sciences Group** (1995–2012) AVIZO® 7.0.1 Konrad-Zuse-Zentrum für
748 Informationstechnik, Berlin (ZIB), Germany.
- 749 **Walker A, Ryan TM, Silcox MT, et al.** (2008) The semicircular canal system and locomotion:
750 the case of extinct lemuroids and lorisooids. *Evol Anth* **17**,135–145.

- 751 **Wible JR, Wang Y, Li C, et al.** (2005) Cranial anatomy and relationships of a new
752 ctenodactyloid (Mammalia, Rodentia) from the early Eocene of Hubei Province, China.
753 *Ann Carnegie Mus* **74**, 91–150.
- 754 **Wilson DE, Reeder DM** (2005) *Mammal Species of the World: A Taxonomic and Geographic*
755 *Reference*, 3rd edn. Baltimore: John Hopkins University.
- 756 **Wood AE** (1937) The mammalian fauna of the White River Oligocene. Part II. Rodentia. *Trans*
757 *Am Philos Soc* **28**, 157–269.
- 758 **Wood AE** (1962) The early Tertiary rodents of the family Paramyidae. *Trans Am Philos Soc* **52**,
759 1–261.
- 760 **Yang A, Hullar TE** (2007) Relationship of Semicircular Canal Size to Vestibular-Nerve
761 Afferent Sensitivity in Mammals. *J Neurophysiol* **98**, 3197-3205.
- 762 **Yi H, Norell MA** (2015) The borrowing origin of modern snakes. *Sci Adv* **1(10)**: e1500743.

763 **Supporting Information**

764 Additional Supporting Information may be found in the online version of this article:

765

766 **Table S1.** Additional information for each specimen including location and date of scanning,
767 source-object distance, energy settings, number of views, interslice spacing/interpixel distance,
768 raw data used to calculate semicircular canal dimensions (see legend), body mass calculations,
769 and locomotor behaviour with references. Under body mass calculations, red indicates specimens
770 for which cheek-tooth area was used instead of skull length. Asterisks indicate specimens for
771 which the right semicircular canals were measured. AMNH, American Museum of Natural

772 History. SMIF, Shared Materials Instrumentation Facility. LSH, Lateral SCC Height. LSW,
773 Lateral SCC Width. PSH, Posterior SCC Height. PSW, Posterior SCC Width. ASH, Anterior
774 SCC Height. ASW, Anterior SCC Width. LSR, Lateral SCC Radius. PSR, Posterior SCC
775 Radius. ASR, Anterior SCC Radius.

776

777 **Table S2.** Data from Figure 4 including log₁₀LSR, log₁₀BM and residuals from the regression
778 of log₁₀LSR and log₁₀BM. Specimens with agility category designations originate from Spoor
779 et al. 2007. Specimens without an agility designation include the extant and fossil rodents
780 examined in this study. Abbreviations: F, fast. M, medium. S, slow.

781

782 **Table S3.** Data from Figure 5 including log₁₀LSR, log₁₀BM and residuals from the regression
783 of log₁₀LSR and log₁₀BM. Specimens with agility category designations originate from Spoor
784 et al. 2007. Specimens without an agility designation include the extant and fossil rodents
785 examined in this study. Abbreviations: F, fast. MF, medium fast. M, medium. MS, medium slow.
786 S, slow. ES, extremely slow.

787

788 **Table S4.** Additional information for each specimen including the angle between the anterior
789 and lateral semicircular canals (ASC/LSC), anterior and posterior semicircular canals
790 (ASC/PSC), and the posterior and lateral semicircular canals (PSC/LSC). The deviation from 90
791 degrees for each angle pair is given as A/L 90VAR for the anterior and lateral semicircular
792 canals, A/P 90VAR for the anterior and posterior semicircular canals, and P/L 90VAR for the
793 posterior and lateral semicircular canals. The average deviation from 90 degrees for all three

794 semicircular canal pairs is given as 90VAR. The logarithm of the angular velocity magnitude
795 logAVM is calculated using the formula from Malinzak et al. 2012.

796

797 **Fig. S1.** Coronal slices from the CT scan data of the right cranium of *Tamiascirus hudsonicus*
798 (USNM 549146) depicts cochlea, anterior semicircular canal (ASC), lateral semicircular canal
799 (LSC) and posterior semicircular canal (PSC).

800

801 **Table legends**

802 **Table 1.** Studies of semicircular canal (SCC) dimensions and vestibular sensitivity in extant
803 taxa. Studies that have analyzed semicircular canal dimensions and vestibular sensitivity in
804 extant taxa are given under Study. Semicircular canal dimensions are the aspect of the SCCs
805 measured in each study in order to determine vestibular sensitivity. The predictive factor is the
806 way in which vestibular sensitivity is quantified as a result of the varying SCC dimensions. The
807 order of the taxa is given under Extant Taxa as well as the number of species used in each order
808 given under Number of Taxa for Spoor et al. (2007) and Pfaff et al. (2015). The species is given
809 for Malinzak et al. (2012) under Extant Taxa.

810

811 **Table 2.** Fossil specimens of eight ischyromyid, two sciurid and two aplodontid rodents used in
812 this study. Fossil rodent specimens including family, subfamily, catalogue number and epoch.
813 Asterisks indicate specimens for which the right semicircular canals were measured.

814

815 **Table 3.** Eighteen additional extant sciurid and aplodontid rodents included in this study with
816 family/subfamily, catalogue number, predicted agility scores from the average semicircular canal
817 radius (SCR) and lateral semicircular canal radius (LSR), and locomotor behaviour. Agility
818 scores are calculated from the all mammal predictive equations from Silcox et al. (2009). The
819 seventeen sciurids span the subfamilies Sciurini, Xerinae, Pteromyini, and Callosciurinae.
820 Asterisks indicate specimens for which the right semicircular canals were measured. References
821 for locomotor behaviour can be found in Table S1. Abbreviations: F, fast. MF, medium fast. M,
822 medium. MS, medium slow.

823
824 **Table 4.** Measurements of semicircular canal angles between each of the ipsilateral canal pairs
825 for fossil and extant rodents with catalogue number. The angle between the anterior and lateral
826 semicircular canals is represented by ASC/LSC, the angle between the anterior and posterior
827 semicircular canals is represented by ASC/PSC, and the angle between the posterior and lateral
828 semicircular canals is represented by PSC/LSC. 90VAR represents the sum of the deviation from
829 90 degrees for all three ipsilateral canal pairs. The logarithm of the angular velocity magnitude
830 ($\log_{10}AVM$) provides an estimate of angular head velocity and is calculated using the formula
831 from Malinzak et al. 2012.

832
833 **Table 5.** Dunn's post-hoc test analyzing the differences in median residuals between the 6
834 agility groups of mammals and extant sciurids. P-values are presented in the upper right half of
835 the table and z statistics are given in the lower left half. Significant differences are highlighted in
836 bold for p-values.

837

838 **Table 6.** Fossil rodent agility scores calculated from average and lateral semicircular canal
839 radius. Agility scores calculated from average semicircular canal radius (SCR) and lateral
840 semicircular canal radius (LSR) for fossil rodents with family, subfamily and catalogue number
841 for each specimen. Agility Category reflects where the specimen falls on the agility scale, ranked
842 by Spoor et al. (2007). Abbreviations: F, fast. MF, medium fast. M, medium. MS, medium slow.

843

844 **Figure legends**

845 **Fig. 1.** Cladogram representing the relationship among the taxa discussed in the text following
846 different studies (Korth and Emry 1991, Mercer and Roth 2003, Hopkins 2008). **A.** Topology
847 based on Meng (1990) and **B.** Section of the cladogram differing based on Asher et al. (2019).
848 The symbol † indicates extinct taxa.

849

850 **Fig. 2.** The anterior semicircular canal of *Heliosciurus rufobrachium* (USNM 378091) after re-
851 slicing of the data in the plane of the canal using the “fit to points” tool in the Slice module of
852 AVIZO 7.0.1. Height and width are shown by the blue and orange arrows respectively. They
853 represent the maximum span of the canal, measured at the center of the lumen. Scale bar = 1mm.

854

855 **Fig. 3.** Bony labyrinth reconstructions for rodents including the extant sciurid *Sciurus*
856 *carolinensis* (AMNH 258346), the extant aplodontid *Aplodontia rufa* (AMNH 42389), two
857 ischyromyids *Paramys delicatus* (AMNH 12506) and *Reithroparamys delicatissimus* (AMNH
858 12561), the fossil sciurid *Cedromus wilsoni* (USNM 256584), and the fossil aplodontid
859 *Prosciurus relictus* (USNM 437793). Each semicircular canal is shown in its respective plane,

860 including the anterior semicircular canal (left), posterior semicircular canal (middle), and the
861 lateral semicircular canal (right). Scale bars represent 1 mm.

862

863 **Fig. 4.** Relationship between body mass (BM) and lateral semicircular canal radius (LSR; A) and
864 the residuals from the least squares regression of $\log_{10}\text{BM}$ and $\log_{10}\text{LSR}$ (B) for fossil and extant
865 rodents in the context of extant rodents from Spoor et al. (2007). The regression line in Part A is
866 calculated using modern specimens and has the following parameters: slope = 0.1595, intercept =
867 -0.24696, and $R^2 = 0.71377$. Modern rodents from Spoor et al. (2007) fall into the fast (e.g.,
868 *Glaucomys volans*; agility score = 6), medium (e.g., *Hydrochaeris hydrochaeris*; agility score =
869 3) and slow (e.g., *Erethizon dorsatum*; agility score = 2) categories. *Aplodontia rufa* generally
870 has small SCCs relative to body mass and groups with rodent taxa in the medium agility
871 category. Convex hulls represent the position of rodents categorized as fast from Spoor et al.
872 (2007; blue) relative to extant sciurids (orange).

873

874 **Fig. 5.** Relationship between body mass (BM) and lateral semicircular canal radius (LSR; A) and
875 the residuals from the least squares regression of $\log_{10}\text{BM}$ and $\log_{10}\text{LSR}$ (B) for fossil and extant
876 rodents in the context of all mammals from Spoor et al. (2007). The regression line in Part A is
877 calculated using modern specimens and has the following parameters: slope = 0.13208, intercept
878 = -0.20602, and $R^2 = 0.71377$. The taxa indicated in Part A include *Sciurus carolinensis* and
879 *Sciurus granatensis*, taxa that group near the fossil sciurids, *Glaucomys volans* which groups
880 near the early fossil aplodontid *Prosciurus relictus*, and *Aplodontia rufa* which groups in a

881 similar agility range to *Mesogaulus paniensis*. The orange convex hull in Part B represents the
882 position of the residuals for extant sciurids.

883

884

885 **Fig. 6.** Boxplot of fossil rodent residuals calculated from the least squares regression of $\log_{10}\text{BM}$
886 and $\log_{10}\text{LSR}$. Fossil rodents fall into three residual categories: 1. low residuals (median = -
887 0.041) and yielding medium slow to medium agility scores, 2. intermediate residuals (median =
888 0.028) yielding medium to medium fast agility scores, and 3. high residuals (median = 0.098)
889 yielding medium fast to fast agility scores.

890

891 **Fig. 7. A.** Relationship between $\log_{10}90\text{VAR}$ and $\log_{10}\text{AVM}$ for fossil and extant rodents in the
892 context of primates and two non-primate species from Malinzak et al. (2012); B. Relationship
893 between $\log_{10}90\text{VAR}$ and the residuals from the least squares regression of $\log_{10}\text{LSR}$ and
894 $\log_{10}\text{BM}$ for fossil and extant rodents.

1 **Table 1.** Studies of semicircular canal (SCC) dimensions and vestibular sensitivity in extant
 2 taxa. Studies that have analyzed semicircular canal dimensions and vestibular sensitivity in
 3 extant taxa are given under Study. Semicircular canal dimensions are the aspect of the SCCs
 4 measured in each study in order to determine vestibular sensitivity. The predictive factor is the
 5 way in which vestibular sensitivity is quantified as a result of the varying SCC dimensions. The
 6 order of the taxa is given under Extant Taxa as well as the number of species used in each order
 7 given under Number of Taxa for Spoor et al. (2007) and Pfaff et al. (2015). The species is given
 8 for Malinzak et al. (2012) under Extant Taxa.

Study	SSC dimensions	Predictive factors	Extant taxa	Number of taxa
Spoor et al. 2007	Radii of curvature	Agility score	Artiodactyla	8
			Carnivora	19
			Chiroptera	7
			Dasyuromorphia	3
			Dermoptera	2
			Didelphimorphia	1
			Diprotodontia	15
			Eulipotyphla	6
			Lagomorpha	2
			Monotremata	1
			Notoryctemorphia	1
			Peramelemorphia	1
			Perissodactyla	2
			Primates	91
			Proboscidae	2
			Rodentia	38
			Scandentia	6
Sirenia	1			
Xenarthra	4			
Pfaff et al. 2015	Multiple dimensions including SSC diameter	SSC sensitivity equation	Chiroptera	3
			Diprotodontia	1
			Eulipotyphla	1
			Notoryctemorphia	1
			Rodentia	43

			Scandentia	1
Malinzak et al. 2012	SSC orthogonality; variance from 90 degrees (90var)	Angular velocity magnitude	<i>Cheirogaleus medius</i>	1
			<i>Daubentonia</i>	
			<i>madagascariensis</i>	1
			<i>Eulemur fulvus</i>	1
			<i>Eulemur mongoz</i>	1
			<i>Galago moholi</i>	1
			<i>Hapalemur griseus</i>	1
			<i>Lemur catta</i>	1
			<i>Microcebus murinus</i>	1
			<i>Nycticebus pygmaeus</i>	1
			<i>Propithecus verreauxi</i>	1
<i>Varecia variegata</i>	1			

- 1 **Table 2.** Fossil specimens of eight ischyromyid, two sciurid and two aplodontid rodents used in this study. Fossil rodent specimens
 2 including family, subfamily, catalogue number and epoch. Asterisks indicate specimens for which the right semicircular canals were
 3 measured.

Family	Subfamily	Species	Catalogue Number	Epoch
Ischyromyidae	Paramyinae	<i>Paramys copei</i> *	AMNH 4756	Early Eocene
	Paramyinae	<i>Paramys delicatus</i>	AMNH 12506	Middle Eocene
	Paramyinae	<i>Pseudotomus oweni</i> *	USNM 17161	Middle Eocene
	Reithroparamyinae	<i>Reithroparamys delicatissimus</i>	AMNH 12561	Middle Eocene
	Reithroparamyinae	<i>Rapamys atramontis</i>	AMNH 128704	Middle Eocene
	Ischyromyinae	<i>Ischyromys typus</i>	AMNH F:AM 144638	Early Oligocene
	Ischyromyinae	<i>Ischyromys typus</i>	ROMV 1007	Early Oligocene
	Ischyromyinae	<i>Titanotheriomys veterior</i>	AMNH 79314	Late Eocene
Sciuridae	Cedromurinae	<i>Cedromus wilsoni</i>	USNM 256584	Early Oligocene
	Sciurinae	<i>Protosciurus cf. rachelae</i>	YPM 14736	Late Oligocene
Aplodontidae	Prosciurinae	<i>Prosciurus relictus</i>	USNM 437793	Early Oligocene
	Mesogaulinae	<i>Mesogaulus paniensis</i>	AMNH F:AM 65511	Early Miocene

1 **Table 3.** Eighteen additional extant sciurid and aplodontid rodents included in this study with family/subfamily/tribe, catalogue
 2 number, predicted agility scores from the average semicircular canal radius (SCR) and lateral semicircular canal radius (LSR), and
 3 locomotor behaviour. The seventeen sciurids span the subfamilies Sciurini, Xerinae, Pteromyini, and Callosciurinae. Asterisks
 4 indicate specimens for which the right semicircular canals were measured. References for locomotor behaviour can be found in Table
 5 S1. Abbreviations: F, fast. MF, medium fast. M, medium. MS, medium slow.

Family/Subfamily/Tribe	Species	Catalogue Number	Agility score from SCR	Agility score from LSR	Agility Category	Locomotor Behaviour
Aplodontidae	<i>Aplodontia rufa</i>	AMNH 42389	2.9	4	MS - M	Fossorial
Sciurini	<i>Sciurus carolinensis</i>	AMNH 258346	5.2	4.7	MF	Arboreal
Sciurini	<i>Tamiasciurus hudsonicus</i>	USNM 549146	5.4	5.7	MF-F	Arboreal
Xerinae	<i>Funisciurus pyrropus</i>	USNM 294865	5.1	5.6	MF-F	Scansorial
Xerinae	<i>Heliosciurus rufobrachium</i>	USNM 378091	5.5	5.4	MF	Arboreal
Xerinae	<i>Paraxerus cepapi</i>	USNM 367956	4.9	5.1	MF	Scansorial
Xerinae	<i>Protoxerus stangeri</i>	USNM 435027	5.1	5.2	MF	Arboreal
Pteromyini	<i>Aeromys tephromelas</i>	USNM 481190	4.9	4.7	MF	Glider
Pteromyini	<i>Glaucomys volans</i>	AMNH 240290	5.6	5.6	F	Glider
Pteromyini	<i>Petaurista petaurista</i>	USNM 589079	5.2	5	MF	Glider
Pteromyini	<i>Hylopetes spadiceus</i>	USNM 488639	4.6	4.7	MF	Glider
Pteromyini	<i>Petinomys setosus</i>	USNM 488674	4.9	4.7	MF	Glider
Pteromyini	<i>Pteromyscus pulverulentus</i>	USNM 481178	5.4	5	MF	Glider
Pteromyini	<i>Pteromys buechneri</i>	USNM 172622	5.2	5.3	MF	Glider
Callosciurinae	<i>Rhinosciurus laticaudatus</i>	USNM 488511	4.4	4.5	M-MF	Terrestrial
Callosciurinae	<i>Callosciurus caniceps</i>	USNM 294865	5.2	6.1	MF-F	Arboreal
Callosciurinae	<i>Lariscus insignis</i> *	USNM 488570	4.9	4.8	MF	Terrestrial
Callosciurinae	<i>Dremomys rufigenis</i> *	USNM 488602	4.6	4.6	MF	Scansorial

For Peer Review Only

1 **Table 4.** Measurements of semicircular canal angles between each of the ipsilateral canal pairs for fossil and extant rodents with
 2 catalogue number. The angle between the anterior and lateral semicircular canals is represented by ASC/LSC, the angle between the
 3 anterior and posterior semicircular canals is represented by ASC/PSC, and the angle between the posterior and lateral semicircular
 4 canals is represented by PSC/LSC. 90VAR represents the sum of the deviation from 90 degrees for all three ipsilateral canal pairs. The
 5 logarithm of the angular velocity magnitude ($\log_{10}AVM$) provides an estimate of angular head velocity and is calculated using the
 6 formula from Malinzak et al. 2012.

Fossil/Extant	Species	Catalogue Number	ASC/LSC	ASC/PSC	PSC/LSC	90VAR	$\log_{10}AVM$
	<i>Aplodontia rufa</i>	AMNH 42389	88	86.2	87.2	8.6	2.35
	<i>Sciurus carolinensis</i>	AMNH 258346	85.3	82.7	85.8	16.2	2.21
	<i>Tamiasciurus hudsonicus</i>	USNM 549146	84.6	83.2	79.5	22.7	2.14
	<i>Funisciurus pyrropus</i>	USNM 294865	79	82.6	84.7	23.7	2.13
	<i>Heliosciurus rufobrachium</i>	USNM 378091	88.4	83.5	88.3	9.8	2.32
	<i>Paraxerus cepapi</i>	USNM 367956	87.5	87	90	5.5	2.45
	<i>Protoxerus stangeri</i>	USNM 435027	76.3	81.8	88.1	23.8	2.13
	<i>Aeromys tephromelas</i>	USNM 481190	89	81.7	83.7	15.6	2.22
Extant	<i>Glaucomys volans</i>	AMNH 240290	78.9	86.4	89.6	15.1	2.23
	<i>Petaurista petaurista</i>	USNM 589079	80.4	85.4	87.8	16.4	2.21
	<i>Hylopetes spadiceus</i>	USNM 488639	82	82.5	96.4	21.9	2.15
	<i>Petinomys setosus</i>	USNM 488674	88.8	85.1	88.6	7.5	2.38
	<i>Pteromyscus pulverulentus</i>	USNM 481178	87.2	86.8	88.5	7.5	2.38
	<i>Pteromys buechneri</i>	USNM 172622	80.7	79.5	97.4	27.2	2.10
	<i>Rhinosciurus laticaudatus</i>	USNM 488511	80.3	88	89.4	12.3	2.27
	<i>Callosciurus caniceps</i>	USNM 294865	81	80.3	93.7	22.4	2.14
	<i>Lariscus insignis</i>	USNM 488570	89.5	81.8	89.4	9.3	2.34

	<i>Dremomys rufigenis</i>	USNM 488602	85	88.3	90.4	7.1	2.40
	<i>Paramys copei</i>	AMNH 4756	88.1	96.3	86.5	11.7	2.29
	<i>Pseudotomus oweni</i>	USNM 17161	77.3	90.7	84.1	19.3	2.17
	<i>Paramys delicatus</i>	AMNH 12506	86.6	92.6	86	10	2.32
	<i>Reithroparamys delicatissimus</i>	AMNH 12561	86.7	89.1	91.9	6.1	2.43
	<i>Rapamys atramontis</i>	AMNH 128704	85.7	85.6	90.5	9.2	2.34
Fossil	<i>Titanotheriomys veterior</i>	AMNH 79314	95.6	97.4	90.7	13.7	2.25
	<i>Ischyromys typus</i>	AMNH F:AM 144638	83.1	82.8	78.6	25.5	2.11
	<i>Ischyromys typus</i>	ROMV 1007	83.6	89.7	88.8	7.9	2.37
	<i>Cedromus wilsoni</i>	USNM 256584	87.1	82.3	87.8	12.8	2.27
	<i>Prosciurus cf. rachelae</i>	YPM 14736	83.6	83.6	84.9	17.9	2.19
	<i>Prosciurus relictus</i>	USNM 437793	81.8	83.8	87.3	17.1	2.20
	<i>Mesogaulus paniensis</i>	AMNH F:AM 65511	94.1	97.8	85.6	16.3	2.21

- 1 **Table 5.** Dunn's post-hoc test analyzing the differences in median residuals between the 6 agility groups of mammals and extant
 2 sciurids. P-values are presented in the upper right half of the table and z statistics are given in the lower left half. Significant
 3 differences are highlighted in bold for p-values.

	Extremely Slow	Slow	Medium Slow	Medium	Medium Fast	Fast	Extant Sciuridae
Extremely Slow		0.1801	0.1589	0.00102	0.001105	5.536x10⁻⁰⁵	1.414x10⁻⁰⁵
Slow	1.341		0.7588	0.0001696	0.001528	2.226x10⁻⁰⁷	6.498x10⁻⁰⁷
Medium Slow	1.409	0.3071		0.02687	0.02561	0.001206	0.000308
Medium	3.285	3.76	2.213		0.5562	0.02782	0.008347
Medium Fast	3.262	3.169	2.232	0.5885		0.4789	0.1276
Fast	4.032	5.179	3.238	2.2	0.7081		0.2178
Extant Sciuridae	4.342	4.976	3.608	2.638	1.523	1.233	

1 **Table 6.** Fossil rodent agility scores calculated from average and lateral semicircular canal radius. Agility scores calculated from
 2 average semicircular canal radius (SCR) and lateral semicircular canal radius (LSR) for fossil rodents with family, subfamily and
 3 catalogue number for each specimen. Agility Category reflects where the specimen falls on the agility scale, ranked by Spoor et al.
 4 (2007). Abbreviations: F, fast. MF, medium fast. M, medium. MS, medium slow.

Family	Subfamily	Species	Catalogue Number	Agility Score from SCR	Agility Score from LSR	Agility Category
	Paramyinae	<i>Paramys copei</i>	AMNH 4756	3.6	3.9	MS - M
	Paramyinae	<i>Paramys delicatus</i>	AMNH 12506	3.4	3.5	MS - M
	Paramyinae	<i>Pseudotomus oweni</i>	USNM 17161	3.1	3.2	MS
Ischyromyidae	Reithroparamyinae	<i>Reithroparamys delicatissimus</i>	AMNH 12561	4.5	4.4	M - MF
	Reithroparamyinae	<i>Rapamys atramontis</i>	AMNH 128704	4.6	4.6	M - MF
	Ischyromyinae	<i>Titanotheriomys veterior</i>	AMNH 79314	4.6	4.6	M - MF
	Ischyromyinae	<i>Ischyromys typus</i>	ROMV 1007	3.4	3.8	MS - M
	Ischyromyinae	<i>Ischyromys typus</i>	AMNH F:AM 144638	4	4	M
Sciuridae	Cedromurinae	<i>Cedromus wilsoni</i>	USNM 256584	5.5	5.3	MF - F
	Sciurinae	<i>Protosciurus cf. rachelae</i>	YPM 14736	5.7	5.4	MF - F
Aplodontidae	Prosciurinae	<i>Prosciurus relictus</i>	USNM 437793	6.1	6.1	F
	Mesogaulinae	<i>Mesogaulus paniensis</i>	AMNH F:AM 65511	4.2	4.1	M

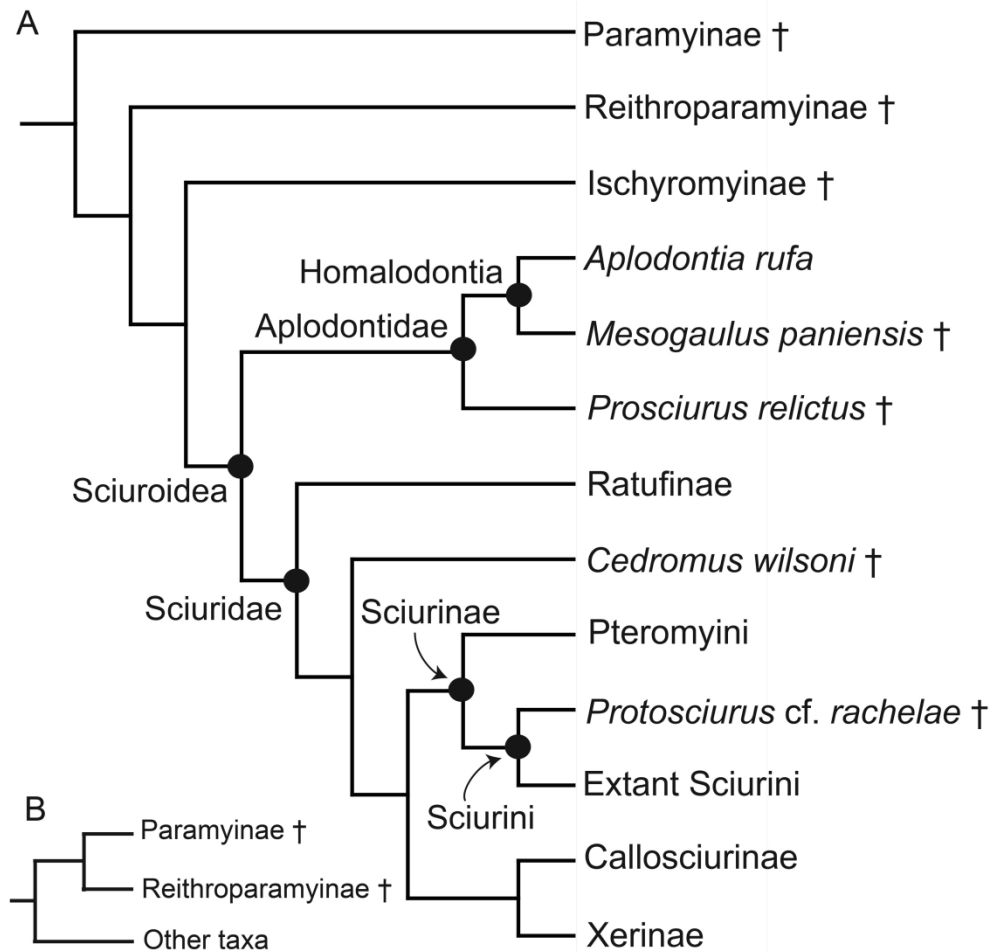


Figure 1. Cladogram representing the relationship among the taxa discussed in the text following different studies (Korth and Emry 1991, Mercer and Roth 2003, Hopkins 2008). A. Topology based on Meng (1990) and B. Section of the cladogram differing based on Asher et al. (2019). The symbol † indicates extinct taxa.

188x181mm (600 x 600 DPI)

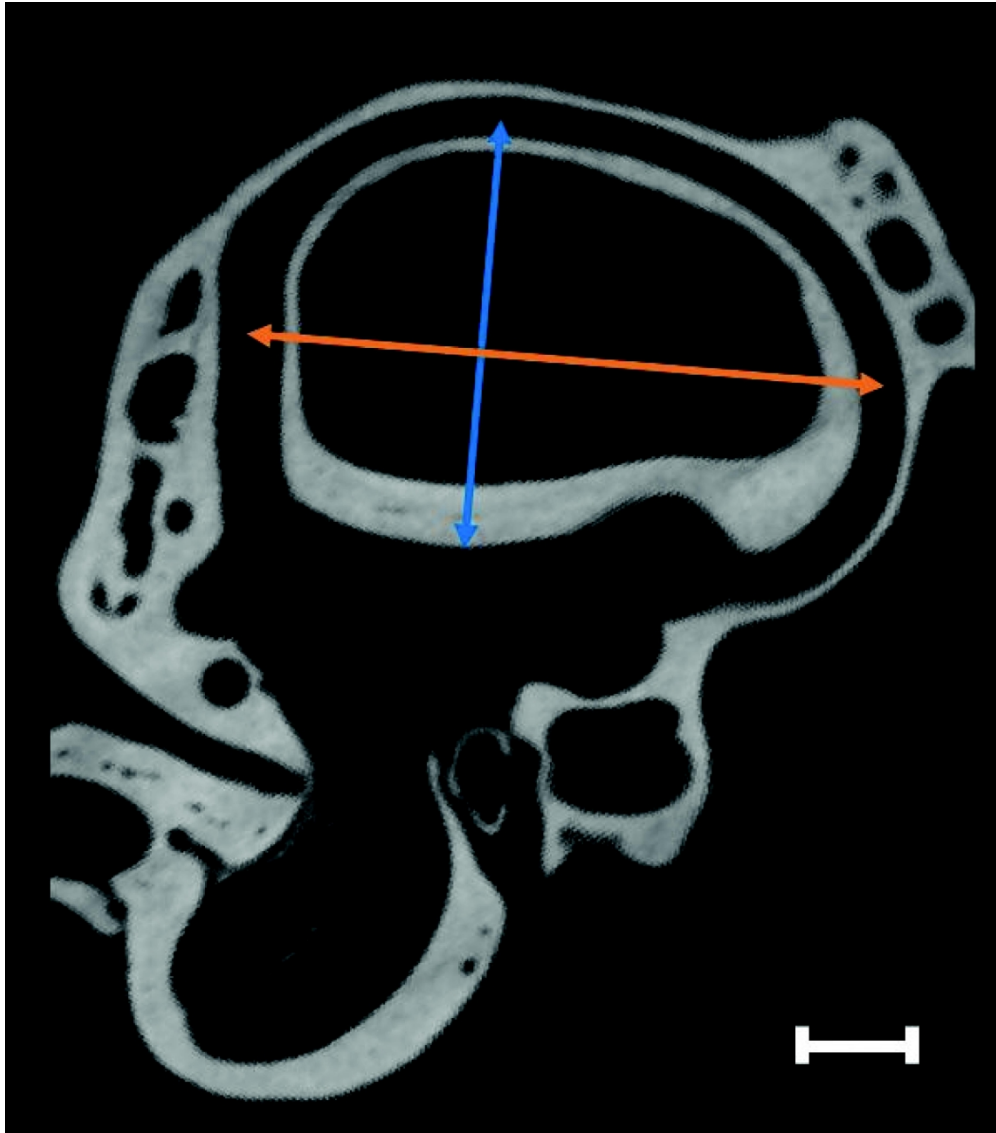


Figure 2. The anterior semicircular canal of *Heliosciurus rufobrachium* (USNM 378091) after re-slicing of the data in the plane of the canal using the “fit to points” tool in the Slice module of AVIZO 7.0.1. Height and width are shown by the blue and orange arrows respectively. Scale bar = 1mm.

158x179mm (600 x 600 DPI)

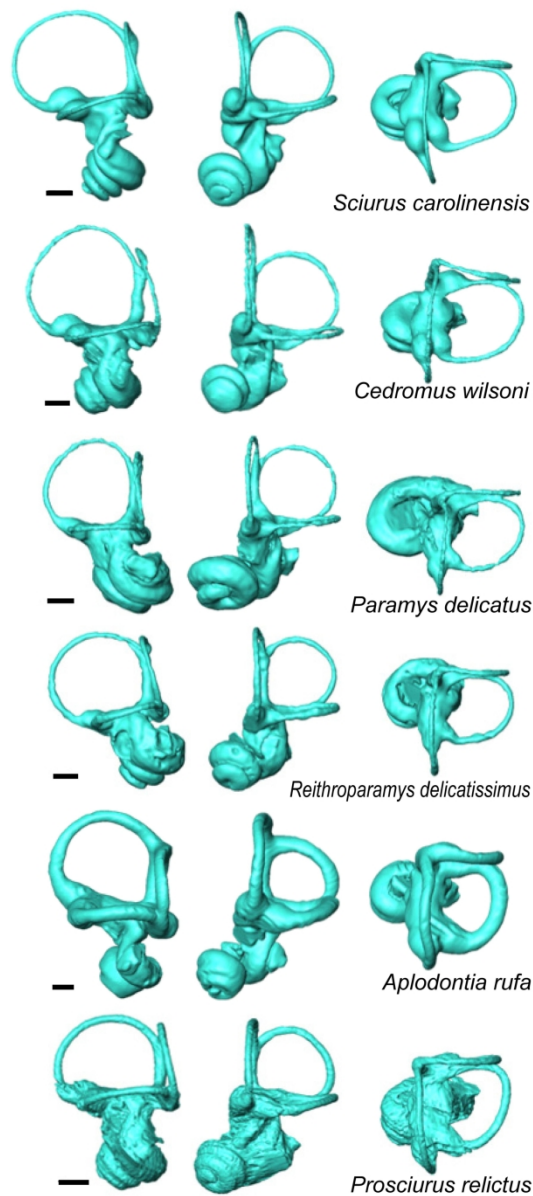


Figure 3. Bony labyrinth reconstructions for rodents including the extant sciurid *Sciurus carolinensis* (AMNH 258346), the extant aplodontid *Aplodontia rufa* (AMNH 42389), two ischyromyids *Paramys delicatus* (AMNH 12506) and *Reithroparamys delicatissimus* (AMNH 12561), the fossil sciurid *Cedromus wilsoni* (USNM 256584), and the fossil aplodontid *Prosciurus relictus* (USNM 437793). Each semicircular canal is shown in its respective plane, including the anterior semicircular canal (left), posterior semicircular canal (middle), and the lateral semicircular canal (right). Scale bars represent 1 mm.

111x254mm (600 x 600 DPI)

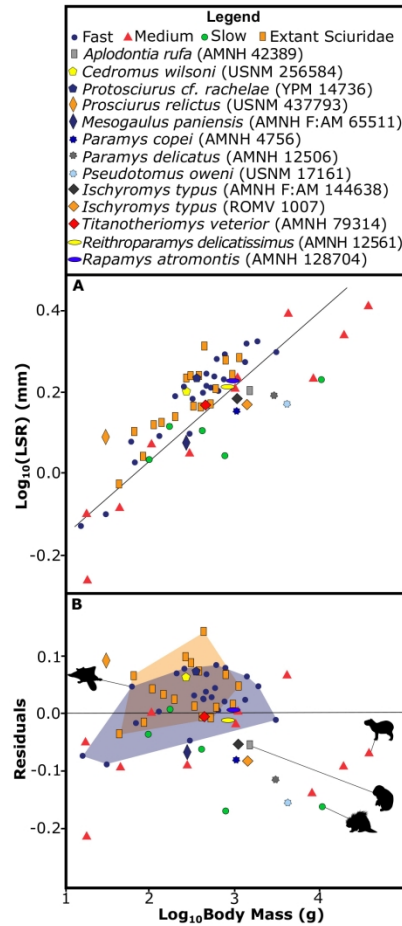


Figure 4. Relationship between body mass (BM) and lateral semicircular canal radius (LSR; A) and the residuals from the least squares regression of $\log_{10}\text{BM}$ and $\log_{10}\text{LSR}$ (B) for fossil and extant rodents in the context of extant rodents from Spoor et al. (2007). The regression line in Part A is calculated using modern specimens and has the following parameters: slope = 0.1595, intercept = -0.24696, and $R^2 = 0.71377$.

Modern rodents from Spoor et al. (2007) fall into the fast (e.g., *Glaucomys volans*; agility score = 6), medium (e.g., *Hydrochaeris hydrochaeris*; agility score = 3) and slow (e.g., *Erethizon dorsatum*; agility score = 2) categories. *Aplodontia rufa* generally has small SCCs relative to body mass and groups with rodent taxa in the medium agility category. Convex hulls represent the position of rodents categorized as fast from Spoor et al. (2007; blue) relative to extant sciurids (orange).

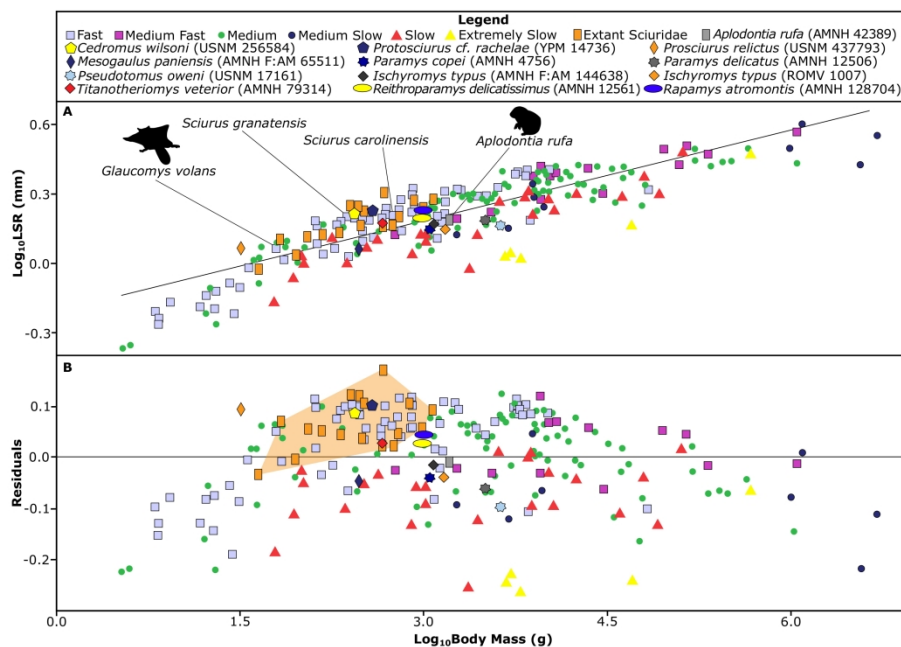


Figure 5. Relationship between body mass (BM) and lateral semicircular canal radius (LSR; A) and the residuals from the least squares regression of $\log_{10}\text{BM}$ and $\log_{10}\text{LSR}$ (B) for fossil and extant rodents in the context of all mammals from Spoor et al. (2007). The regression line in Part A is calculated using modern specimens and has the following parameters: slope = 0.13208, intercept = -0.20602, and $R^2 = 0.71377$. The taxa indicated in Part A include *Sciurus carolinensis* and *Sciurus granatensis*, taxa that group near the fossil sciurids, *Glaucomys volans* which groups near the early fossil aplodontid *Prosciurus relictus*, and *Aplodontia rufa* which groups in a similar agility range to *Mesogaulus paniensis*. The orange convex hull in Part B represents the position of the residuals for extant sciurids.

279x215mm (600 x 600 DPI)

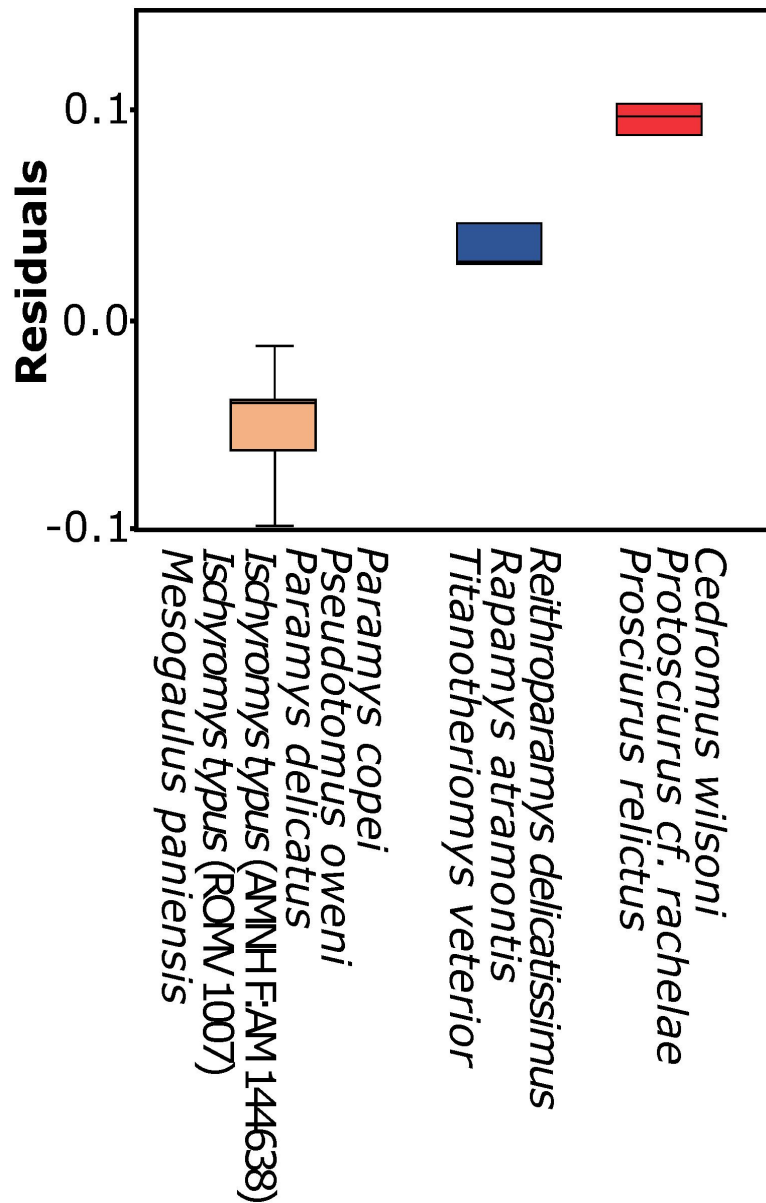


Figure 6. Boxplot of fossil rodent residuals calculated from the least squares regression of $\log_{10}BM$ and $\log_{10}LSR$. Fossil rodents fall into three residual categories: 1. low residuals (median = -0.041) and yielding medium slow to medium agility scores, 2. intermediate residuals (median = 0.028) yielding medium to medium fast agility scores, and 3. high residuals (median = 0.098) yielding medium fast to fast agility scores.

64x100mm (600 x 600 DPI)

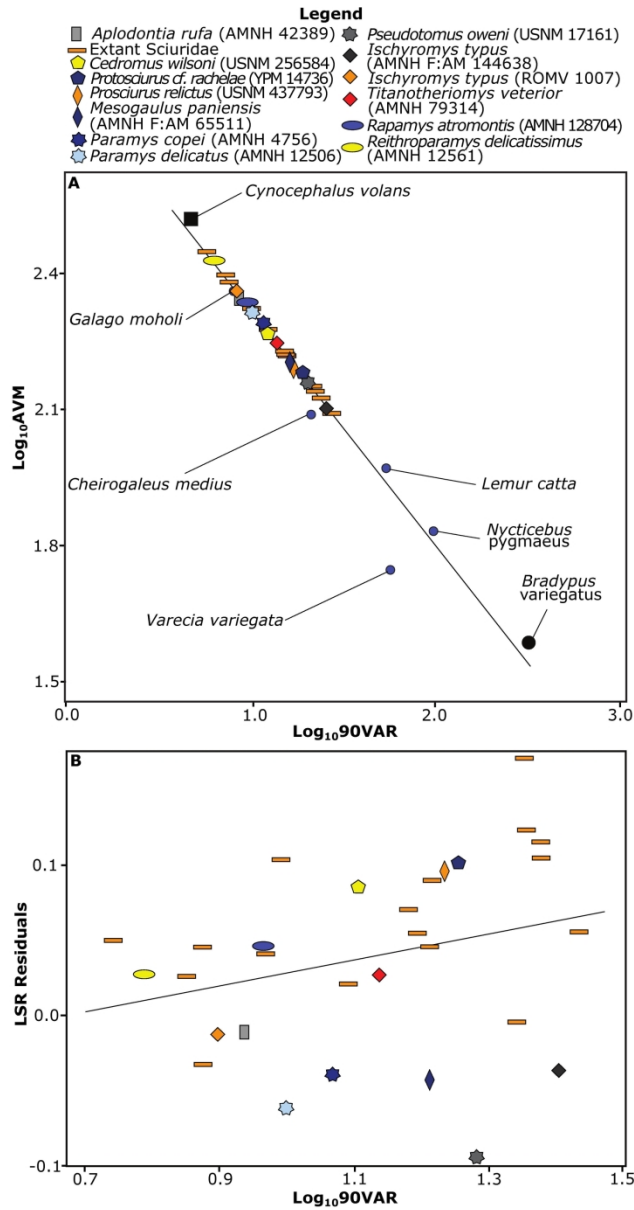


Figure 7. A. Relationship between $\log_{10}90VAR$ and $\log_{10}AVM$ for fossil and extant rodents in the context of primates and two non-primate species from Malinzak et al. (2012); B. Relationship between $\log_{10}90VAR$ and the residuals from the least squares regression of $\log_{10}LSR$ and $\log_{10}BM$ for fossil and extant rodents.

141x268mm (300 x 300 DPI)

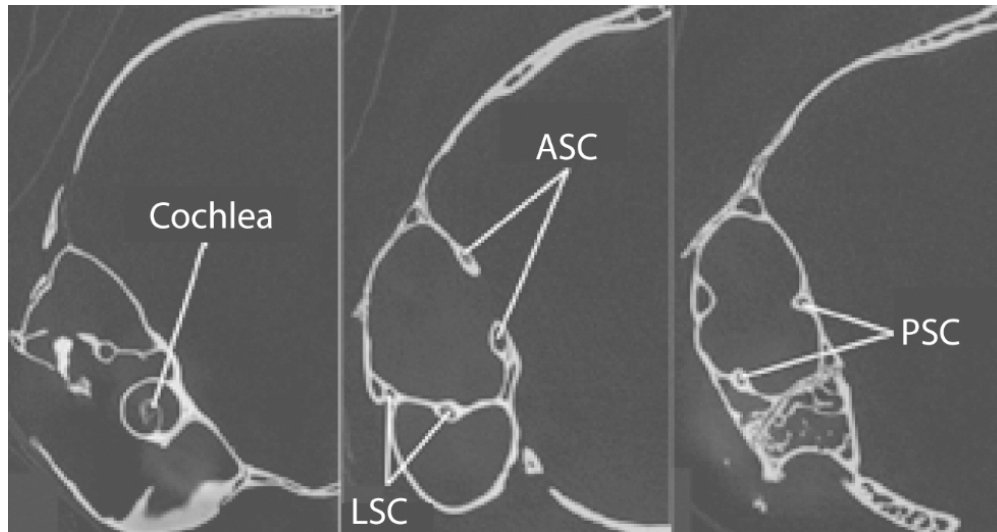


Figure S1. Coronal slices from the CT scan data of the right cranium of *Tamiascirus hudsonicus* (USNM 549146) depicts cochlea, anterior semicircular canal (ASC), lateral semicircular canal (LSC) and posterior semicircular canal (PSC).

113x59mm (220 x 220 DPI)

Evolution of arboreality a

For Peer Review Only

¹Department of Anthro

²School of GeoS

Journal of Anatomy

SUPPORTING TABLES

**and fossoriality in squirrels and aplodontid rodents: insi
semicircular canals of fossil rodents**

Raj Bhagat¹, Ornella C. Bertrand², Mary T. Silcox¹

[Corresponding author: raj.bhagat@mail.utoronto.ca](mailto:raj.bhagat@mail.utoronto.ca)

opology, University of Toronto Scarborough, Toronto, ON M1C 1A4, Ca
Sciences, University of Edinburgh, Grant Institute, Edinburgh, Scotland,

ights from the

anada
UK

For Peer Review Only

Table S1. Additional information for each specimen including location and date of scanning, so area was used instead of skull length. Asterisks indicate specimens for which the right semicirc Radius. PSR, Posterior SSC Radius. ASR, Anterior SSC Radius.

	Specimen	Catalogue Number	Location and Date of Scanning
	<i>Paramys copei</i> *	AMNH 4756	AMNH - 2013
	<i>Paramys delicatus</i>	AMNH 12506	AMNH - 2013
	<i>Pseudotomus oweni</i> *	USNM 17161	SMIF - 2014
	<i>Reithroparamys delicatissimus</i>	AMNH 12561	AMNH - 2013
	<i>Rapamys atramontis</i>	AMNH 128704	AMNH - 2013
Fossil	<i>Ischyromys typus</i>	AMNH F:AM 144638	AMNH - 2015
	<i>Ischyromys typus</i>	ROMV 1007	SMIF - 2013
	<i>Titanotheriomys veterior</i>	AMNH 79314	AMNH - 79314
	<i>Cedromus wilsoni</i>	USNM 256584	SMIF - 2014
	<i>Protosciurus cf. rachelae</i>	YPM 14736	SMIF - 2014
	<i>Prosciurus relictus</i>	USNM 437793	SMIF - 2014
	<i>Mesogaulus paniensis</i>	AMNH F:AM 65511	AMNH - 2015
	<i>Aplodontia rufa</i>	AMNH 42389	SMIF - 2013
	<i>Sciurus carolinensis</i>	AMNH 258346	SMIF -2013
	<i>Tamiasciurus hudsonicus</i>	USNM 549146	SMIF - 2014
	<i>Funisciurus pyrropus</i>	USNM 294865	SMIF - 2014
	<i>Heliosciurus rufobrachium</i>	USNM 378091	SMIF - 2014
	<i>Paraxerus cepapi</i>	USNM 367956	SMIF - 2014
	<i>Protoxerus stangeri</i>	USNM 435027	SMIF - 2014
	<i>Aeromys tephromelas</i>	USNM 481190	SMIF - 2014
Extant	<i>Glaucomys volans</i>	AMNH 240290	SMIF -2013
	<i>Petaurista petaurista</i>	USNM 589079	SMIF - 2014
	<i>Hylopetes spadiceus</i>	USNM 488639	SMIF - 2014
	<i>Petinomys setosus</i>	USNM 488674	SMIF - 2014
	<i>Pteromyscus pulverulentus</i>	USNM 481178	SMIF - 2014
	<i>Pteromys buechneri</i>	USNM 172622	SMIF - 2014
	<i>Rhinosciurus laticaudatus</i>	USNM 488511	SMIF - 2014
	<i>Callosciurus caniceps</i>	USNM 294865	SMIF - 2014
	<i>Lariscus insignis</i> *	USNM 488570	SMIF - 2014
	<i>Dremomys rufigenis</i> *	USNM 488602	SMIF - 2014

source-object distance, energy settings, number of views, interslice spacing/interpixel distance, raw data. All data were measured. AMNH, American Museum of Natural History. SMIF, Shared Materials I

Source-object Distance (mm)	Energy settings mA	kv	Number of views	Interslice spacing/interpixel distance (mm)
158.79	170	180	1500	0.039046
144.74	170	180	2150	0.035591
265.08	165	88	1650	0.056952
176.94	180	240	1500	0.043510
175.87	170	180	1580	0.043247
166.75	170	220	1500	0.041057
229.08	155	186	2300	0.039463
-	-	-	-	0.035560
113.87	165	88	1600	0.026133
111.98	170	100	1800	0.028292
77.34	165	98	1650	0.016195
196.29	220	150	1500	0.048330
239.82	145	160	2700	0.041313
187.80	120	175	2100	0.032352
119.96	150	98	1700	0.025826
122.09	255	55	1800	0.026453
130.89	225	55	1800	0.028359
102.24	150	98	1700	0.022011
158.79	225	55	1800	0.034404
170.24	225	55	1800	0.036885
107.46	105	165	2775	0.018512
170.24	225	55	1800	0.036885
93.89	160	119	1700	0.020213
82.87	150	98	1700	0.017841
113.53	150	98	1700	0.024442
96.69	160	119	1700	0.020816
143.25	150	98	1700	0.030840
144.07	150	98	1700	0.031016
132.25	150	980	1700	0.028471
140.03	150	98	1700	0.030147

ta used to calculate semicircular canal dimensions (see legend), body mass calculations, and locomot Instrumentation Facility. LSH, Lateral SSC Height. LSW, Lateral SSC Width. PSH, Posterior SSC H

LSH	LSW	PSH	PSW	ASH	ASW	LSR	PSR	ASR	SCR
3.027	2.659	3.03	2.88	3.391	3.543	1.4215	1.4575	1.7335	1.5375
2.951	3.264	3.314	3.543	3.88	4.317	1.55375	1.71425	2.04925	1.77242
2.842	3.086	3.311	3.453	3.464	4.017	1.482	1.691	1.87025	1.68108
3.176	3.283	3.379	3.26	4.082	4.698	1.61475	1.65975	2.195	1.82317
3.779	3.038	3.446	3.703	4.302	4.544	1.70425	1.78725	2.2115	1.901
2.546	3.559	3.25	2.976	3.472	4.655	1.52625	1.5565	2.03175	1.70483
2.601	3.311	2.91	2.228	2.979	3.856	1.478	1.2845	1.70875	1.49042
2.855	3.061	2.802	3.427	3.253	4.333	1.479	1.55725	1.8965	1.64425
3.311	3.06	3.24	3.402	4.155	4.736	1.59275	1.6605	2.22275	1.8253
3.658	3.176	3.847	3.768	4.518	4.632	1.7085	1.90375	2.2875	1.96658
2.272	2.602	2.427	2.582	2.386	3.449	1.2185	1.25225	1.45875	1.30983
2.68	2.483	2.125	2.588	2.926	3.451	1.17825	1.29075	1.59425	1.3544
1.877	2.633	2.14	2.81	2.77	3.605	1.59375	1.2375	1.1275	1.319583
4.652	3.412	3.27	3.17	4.005	5.485	1.6115	2.016	2.3725	2
3.087	3.792	2.772	3.225	3.566	4.855	1.71975	1.49925	2.10525	1.77475
3.176	3.727	2.983	3.16	3.437	4.224	1.72575	1.53575	1.91525	1.725583
2.968	3.898	3.727	4.191	3.456	4.847	1.7165	1.9795	2.07575	1.923917
2.411	2.949	2.376	2.655	2.881	3.548	1.34	1.25775	1.60725	1.401667
3.755	3.876	3.865	3.886	4.32	5.212	1.90775	1.93775	2.383	2.076167
3.455	3.488	3.569	4.057	4.553	5.423	1.73575	1.9065	2.494	2.045417
2.411	2.663	2.556	2.621	2.757	3.603	1.2685	1.29425	1.59	1.38425
3.657	4.073	4.22	4.558	4.827	5.777	1.9325	2.1945	2.651	2.259333
1.848	2.581	2.005	2.157	2.455	3.35	1.10725	1.0405	1.45125	1.199667
1.733	2.047	2.016	2.21	2.58	2.93	0.945	1.0565	1.3775	1.126333
2.589	2.962	3.452	4.149	3.381	3.64	1.38775	1.90025	1.75525	1.681083
2.432	2.816	2.755	3.128	2.616	3.419	1.312	1.47075	1.50875	1.4305
2.78	3.175	2.849	3.212	3.401	4.328	1.48875	1.51525	1.93225	1.645417
3.51	4.743	3.017	3.353	3.265	4.572	2.06325	1.5925	1.95925	1.871667
2.656	3.219	3.379	3.297	3.372	4.308	1.46875	1.669	1.92	1.685917
2.824	3.05	2.96	3.253	3.436	4.101	1.4685	1.55325	1.88425	1.635333

for behaviour with
eight. PSW, Postc

Body Mass (g)

1029.89
2913.82
3911.71
856
918.932649
1109.01
1342.23
434.263
268.89
349.616
30.075
266.48
1475.86
592.55
256.61
301.15
354.98
138.13
767.23
904.59
63.97
1096.65
84.22
41.86
195.44
106.37
507.38
437.35
324.71
418.43

For Peer Review Only

references. Under body mass calculations, red indicates specimens for which cheek-tooth anterior SSC Width. ASH, Anterior SSC Height. ASW, Anterior SSC Width. LSR, Lateral SSC

Locomotor Behaviour

Scansorial (Rose and Chinnery, 2004)
Scansorial (Rose and Chinnery, 2004)
Fossorial (Dunn and Rasmussen, 2007)
Arboreal (Wood, 1962)
Terrestrial (Bertrand et al., 2016)
Fossorial (Wood, 1937)
Fossorial (Wood, 1937)
Terrestrial (Bertrand et al., 2016a)
Arboreal (Hypothesized; see Bertrand et al., 2017)
Arboreal (Korth and Samuels, 2015)
Arboreal (Hopkins, 2005; 2008)
Fossorial (Hopkins, 2005; 2008)
Fossorial (Hopkins, 2005; 2008)
Arboreal (Reid, 2006)
Arboreal (Reid, 2006)
Scansorial (Kingdon, 1974)
Arboreal (Kingdon, 1974)
Scansorial (Kingdon, 1974)
Arboreal (Kingdon, 1974; Thorington et al., 2012)
Glider (Thorington et al., 2012)
Glider (Reid, 2006)
Glider (Francis, 2008; Smith and Xie, 2013; Thorington et al., 2012)
Glider (Nowak, 1999)
Glider (Thorington et al., 2012)
Glider (Nowak, 1999)
Glider (Thorington et al., 2012)
Terrestrial (Nowak, 1999; Francis, 2008)
Arboreal (Nowak, 1999)
Terrestrial (Francis, 2008; Thorington et al., 2012)
Scansorial (Francis, 2008; Nowak, 1999)

Table S2. Data from Figure 4 including log10LSR, log10BM and residuals from the regression. Specimens with agility category designations originate from Spoor et al. 2007. Specimens are the extant and fossil rodents examined in this study. Abbreviations: F, fast. M, medium. S, slow.

Species	log10BM	log10LSR
<i>Anomalurus derbianus</i>	2.656	0.215
<i>Castor canadensis</i>	4.271	0.343
<i>Cavia porcellus</i>	3	0.216
<i>Chinchilla laniger</i>	2.653	0.245
<i>Cryptomys hottentotus natalensis</i>	1.978	0.033
<i>Cryptomys mehowi</i>	2.602	0.107
<i>Dipus sagitta</i>	1.82	0.026
<i>Erethizon dorsatum</i>	4.026	0.232
<i>Glaucomys volans</i>	1.774	0.081
<i>Hydrochaeris hydrochaeris (Hydrochoerus capybara)</i>	4.597	0.419
<i>Idiurus macrotis</i>	1.477	-0.098
<i>Idiurus zenkeri</i>	1.197	-0.13
<i>Lophiomys imhausi</i>	2.878	0.043
<i>Marmota monax</i>	3.61	0.396
<i>Meriones unguiculatus</i>	2	0.074
<i>Microtus pennsylvanicus</i>	1.633	-0.081
<i>Mus musculus</i>	1.276	-0.257
<i>Myocastor coypus</i>	3.895	0.235
<i>Ondatra zibethicus</i>	2.998	0.235
<i>Pedetes capensis</i>	3.484	0.298
<i>Peromyscus maniculatus</i>	1.229	-0.101
<i>Petaurista petaurista</i>	3.267	0.322
<i>Rattus norvegicus</i>	2.431	0.05
<i>Ratufa bicolor</i>	3.138	0.317
<i>Ratufa macroura</i>	3.112	0.273
<i>Sciurus aberti</i>	2.78	0.28
<i>Sciurus carolinensis</i>	2.711	0.213
<i>Sciurus granatensis</i>	2.398	0.213
<i>Sciurus niger</i>	2.877	0.289
<i>Sciurus richmondi</i>	2.301	0.19
<i>Sciurus vulgaris</i>	2.507	0.183
<i>Spalax ehrenbergi</i>	2.23	0.117
<i>Spermophilus beecheyi</i>	2.791	0.205
<i>Spermophilus parryi</i>	2.872	0.231
<i>Spermophilus richardsoni</i>	2.461	0.098
<i>Spermophilus tridecemlineatus</i>	2.1	0.091
<i>Xerus erythropus</i>	2.76	0.238
<i>Xerus rutilus</i>	2.623	0.197
<i>Aplodontia rufa</i>	3.169	0.20242
<i>Sciurus carolinensis</i>	2.7727	0.20723
<i>Tamiasciurus hudsonicus</i>	2.4093	0.23547
<i>Funisciurus pyrropus</i>	2.4788	0.23698
<i>Heliosciurus rufobrachium</i>	2.5502	0.23464

<i>Paraxerus cepapi</i>	2.1403	0.1271
<i>Protoxerus stangeri</i>	2.8849	0.28052
<i>Aeromys tephromelas</i>	2.9565	0.23949
<i>Glaucomys volans</i>	1.806	0.10329
<i>Petaurista petaurista</i>	3.0401	0.28612
<i>Hylopetes spadiceus</i>	1.9254	0.044246
<i>Petinomys setosus</i>	1.6218	-0.024568
<i>Pteromyscus pulverulentus</i>	2.291	0.14231
<i>Pteromys buechneri</i>	2.0268	0.11793
<i>Rhinosciurus laticaudatus</i>	2.7053	0.17282
<i>Callosciurus caniceps</i>	2.6408	0.31455
<i>Lariscus insignis</i>	2.5115	0.16695
<i>Dremomys rufigenis</i>	2.6216	0.16687
<i>Paramys copei</i>	3.0128	0.15275
<i>Paramys delicatus</i>	3.4645	0.19138
<i>Pseudotomus oweni</i>	3.5924	0.17085
<i>Reithroparamys delicatissimus</i>	2.9325	0.20811
<i>Rapamys atramontis</i>	2.9633	0.23153
<i>Ischyromys typus</i> ROMV 1007	3.0449	0.18363
<i>Ischyromys typus</i> AMNH F:AM 144638	3.1278	0.16967
<i>Titanotheriomys veterior</i>	2.6378	0.16997
<i>Cedromus wilsoni</i>	2.4296	0.20215
<i>Protosciurus cf. rachelae</i>	2.5436	0.23261
<i>Prosciurus relictus</i>	1.4782	0.085826
<i>Mesogaulus paniensis</i>	2.4257	0.071237

ression of log₁₀LSR and log₁₀BM.
 is without an agility designation include
 S, slow.

Agility Category	Residual
F	0.038324
M	-0.091269
M	-0.015544
F	0.068803
S	-0.035534
S	-0.061063
F	-0.017333
S	-0.16319
F	0.045004
M	-0.067267
F	-0.086624
F	-0.073964
S	-0.16908
M	0.067161
M	0.0019567
M	-0.094507
M	-0.21356
M	-0.1393
M	0.003775
F	-0.010742
M	-0.050068
F	0.047869
M	-0.090788
F	0.063445
F	0.023592
F	0.083546
F	0.027552
F	0.077475
F	0.077075
F	0.069947
F	0.03009
S	0.0082715
F	0.0067916
F	0.019872
F	-0.047573
F	0.0030066
F	0.044736
F	0.025588
-	-0.056087
-	0.011937
-	0.098143
-	0.088568
-	0.074843

-	0.032685
-	0.067332
-	0.014889
-	0.062194
-	0.048185
-	-0.015901
-	-0.036288
-	0.023851
-	0.041613
-	-0.011723
-	0.1403
-	0.013321
-	-0.0043187
-	-0.0808316
-	-0.11424775
-	-0.1551778
-	-0.01266375
-	0.00584365
-	-0.05507155
-	-0.0822541
-	-0.0037991
-	0.0615888
-	0.0738658
-	0.0970131
-	-0.06870215

For Review Only

Table S3. Data from Figure 5 including log₁₀LSR, log₁₀BM and residuals from the regression of log₁₀BM. Specimens with agility category designations originate from Spoor et al. 2007. Specimens designation include the extant and fossil rodents examined in this study. Abbreviations: F, fast. MF, n medium. MS, medium slow. S, slow. ES, extremely slow.

Species	log ₁₀ BM	log ₁₀ LSR	Agility Category
<i>Bos taurus</i>	5.462	0.447	M
<i>Camelus dromedarius</i>	5.618	0.495	M
<i>Gazella bennetti</i>	4.362	0.321	M
<i>Giraffa camelopardalis</i>	5.952	0.502	MS
<i>Hippopotamus amphibius</i>	6.057	0.606	MS
<i>Oryx beisa (gazella)</i>	5.298	0.424	M
<i>Ovis aries</i>	4.528	0.273	M
<i>Sus scrofa</i>	4.74	0.258	M
<i>Canis familiaris</i>	4.141	0.305	M
<i>Enhydra lutris</i>	4.432	0.318	MF
<i>Felis catus</i>	3.556	0.228	M
<i>Felis concolor</i>	4.751	0.34	MF
<i>Herpestes ichneumon (griseus)</i>	3.474	0.185	M
<i>Lutra lutra</i>	3.912	0.28	MF
<i>Lynx rufus</i>	3.989	0.314	M
<i>Mustela nivalis (Putorius vulgaris)</i>	1.94	0.013	M
<i>Nyctereutes procyonoideus viverrinus</i>	3.653	0.158	MS
<i>Panthera leo</i>	5.172	0.5	M
<i>Panthera tigris</i>	5.176	0.451	M
<i>Procyon cancrivorus</i>	3.845	0.308	MS
<i>Proteles cristatus</i>	3.932	0.251	MS
<i>Taxidea taxus</i>	3.857	0.352	MS
<i>Vulpes vulpes</i>	3.699	0.267	M
<i>Halichoerus grypus</i>	5.288	0.477	MF
<i>Odobenus rosmarus</i>	6.006	0.577	MF
<i>Phoca groenlandica (Pagophilus groenlandicus)</i>	5.106	0.512	MF
<i>Phoca vitulina</i>	4.91	0.495	MF
<i>Eptesicus fuscus</i>	1.274	-0.113	F
<i>Myotis lucifugus</i>	0.91	-0.162	F
<i>Myotis macrodactylus</i>	0.813	-0.251	F
<i>Nyctalus lasiopterus aviator</i>	1.542	-0.007	F
<i>Pipistrelles pipistrelles</i>	0.816	-0.226	F
<i>Pteropus giganteus</i>	3.07	0.118	F
<i>Rhinolophus cornutus cornutus</i>	0.785	-0.2	F
<i>Phascogale tapoatafa (Phascologale penicillata)</i>	2.236	0.075	F
<i>Sminthopsis laniger (Antechinomys lanigera)</i>	1.398	-0.074	F
<i>Sminthopsis macroura (S. larapinta)</i>	1.266	-0.183	F
<i>Cynocephalus variegatus</i>	3.138	0.222	F
<i>Cynocephalus volans</i>	3	0.221	F
<i>Didelphis virginiana</i>	3.341	-0.018	S
<i>Acrobates pygmaeus</i>	1.157	-0.182	F
<i>Ailurops ursinus</i>	3.845	0.207	S

<i>Cercartetus nanus</i>	1.425	-0.209	F
<i>Dactylopsila trivirgata</i>	2.556	0.122	F
<i>Hemibelideus lemuroides</i>	2.985	0.102	S
<i>Macropus fuliginosus (melanops)</i>	4.797	0.327	F
<i>Petauroides volans</i>	3.114	0.184	F
<i>Petaurus breviceps</i>	2.146	0.043	F
<i>Petaurus norfolcensis</i>	2.362	0.041	F
<i>Petrogale penicillata</i>	3.823	0.194	F
<i>Phalanger orientalis</i>	3.398	0.124	S
<i>Phascolarctos cinereus</i>	3.842	0.309	S
<i>Pseudocheirus peregrinus</i>	2.893	0.182	M
<i>Spilocuscus maculatus</i>	3.581	0.277	S
<i>Trichosurus vulpecula</i>	3.533	0.194	M
<i>Blarina brevicauda</i>	1.201	-0.209	M
<i>Erinaceus europaeus</i>	2.934	0.086	M
<i>Scalopus aquaticus</i>	1.908	-0.066	S
<i>Sorex cinereus</i>	0.577	-0.349	M
<i>Sorex hoyi</i>	0.519	-0.362	M
<i>Talpa europaea</i>	1.989	0.009	S
<i>Lepus europaeus</i>	3.522	0.227	MF
<i>Oryctolagus cuniculus</i>	3.241	0.202	MF
<i>Ornithorhynchus anatinus</i>	3.243	0.157	M
<i>Notoryctes typhlops</i>	1.74	-0.163	S
<i>Isoodon obesulus (Perameles obesula)</i>	3.025	0.063	M
<i>Diceros bicornis</i>	6	0.441	M
<i>Equus caballus</i>	5.398	0.444	M
<i>Alouatta seniculus</i>	3.826	0.303	S
<i>Aotus trivirgatus</i>	2.889	0.261	MF
<i>Arctocebus calabarensis</i>	2.494	0.075	S
<i>Ateles geoffroyi</i>	3.877	0.32	M
<i>Avahi laniger</i>	3.07	0.216	F
<i>Cacajao calvus</i>	3.5	0.289	M
<i>Cacajao melanocephalus</i>	3.433	0.29	M
<i>Callicebus moloch</i>	3.009	0.241	M
<i>Callicebus torquatus</i>	3.095	0.277	M
<i>Callimico goeldi</i>	2.727	0.128	MF
<i>Callithrix jacchus</i>	2.51	0.165	F
<i>Cebus apella</i>	3.489	0.275	M
<i>Cercocebus torquatus atys</i>	3.792	0.386	F
<i>Cercopithecus cephus</i>	3.632	0.347	M
<i>Cercopithecus diana</i>	3.716	0.385	F
<i>Cercopithecus mitis</i>	3.899	0.403	M
<i>Cercopithecus mona</i>	3.708	0.364	M
<i>Cercopithecus nictitans</i>	3.738	0.392	M
<i>Cheirogaleus major</i>	2.602	0.145	M
<i>Cheirogaleus medius</i>	2.416	0.089	M
<i>Chlorocebus aethiops</i>	3.613	0.355	M
<i>Colobus guereza</i>	3.99	0.39	MF
<i>Colobus polykomos</i>	3.959	0.407	M

<i>Daubentonia madagascariensis</i>	3.407	0.3	F
<i>Erythrocebus patas</i>	3.975	0.408	F
<i>Eulemur fulvus ssp.</i>	3.332	0.298	M
<i>Eulemur macaco</i>	3.378	0.306	M
<i>Eulemur mongoz</i>	3.206	0.308	M
<i>Galago elegantulus</i>	2.46	0.221	F
<i>Galago moholi</i>	2.272	0.172	F
<i>Galago senegalensis</i>	2.342	0.203	F
<i>Galagoides alleni</i>	2.442	0.202	F
<i>Galagoides demidoff</i>	1.789	0.096	M
<i>Gorilla gorilla</i>	5.083	0.485	S
<i>Hapalemur griseus</i>	3.038	0.271	M
<i>Hapalemur simus</i>	3.237	0.329	F
<i>Homo sapiens</i>	4.766	0.346	M
<i>Hylobates hoolock</i>	3.838	0.386	F
<i>Hylobates klossii</i>	3.754	0.392	F
<i>Hylobates lar</i>	3.75	0.381	F
<i>Hylobates moloch</i>	3.818	0.402	F
<i>Hylobates pileatus</i>	3.736	0.402	F
<i>Hylobates syndactylus</i>	4.053	0.415	M
<i>Indri indri</i>	3.802	0.384	F
<i>Lagothrix lagotricha</i>	3.867	0.301	MS
<i>Lemur catta</i>	3.344	0.284	M
<i>Leontopithecus rosalia</i>	2.792	0.148	F
<i>Lepilemur sp.</i>	2.883	0.233	F
<i>Lophocebus albigena</i>	3.916	0.431	MF
<i>Loris tardigradus</i>	2.342	0.007	S
<i>Macaca cyclopis</i>	3.738	0.371	M
<i>Macaca fascicularis</i>	3.651	0.345	M
<i>Macaca fuscata</i>	3.978	0.359	M
<i>Macaca mulatta</i>	3.968	0.385	M
<i>Macaca nemestrina</i>	3.89	0.312	M
<i>Macaca nigra</i>	3.885	0.371	M
<i>Macaca sylvanus</i>	4.132	0.397	M
<i>Macaca tonkeana</i>	4.077	0.377	M
<i>Mandrillus sphinx</i>	4.5	0.415	M
<i>Microcebus murinus</i>	1.841	0.077	M
<i>Microcebus rufus</i>	1.628	0.029	M
<i>Nasalis larvatus</i>	4.31	0.423	MF
<i>Nycticebus coucang</i>	2.933	0.127	S
<i>Otolemur crassicaudatus</i>	3.061	0.241	M
<i>Otolemur garnetti</i>	2.883	0.276	F
<i>Pan paniscus</i>	4.592	0.374	M
<i>Pan troglodytes</i>	4.653	0.398	M
<i>Papio hamadryas z</i>	4.223	0.428	M
<i>Perodicticus potto</i>	2.993	0.134	S
<i>Pithecia pithecia</i>	3.288	0.293	M
<i>Pongo pygmaeus</i>	4.755	0.38	S
<i>Procolobus badius</i>	3.934	0.32	M

<i>Propithecus diadema</i>	3.785	0.375	F
<i>Propithecus verreauxi</i>	3.561	0.336	F
<i>Pygathrix nemaeus</i>	4.041	0.399	MF
<i>Saguinus oedipus</i>	2.621	0.182	F
<i>Saimiri sciureus</i>	2.88	0.253	F
<i>Semnopithecus entellus</i>	4.162	0.377	M
<i>Tarsius bancanus</i>	2.088	0.186	F
<i>Tarsius syrichta</i>	2.099	0.169	F
<i>Theropithecus gelada</i>	4.219	0.344	M
<i>Trachypithecus obscurus</i>	3.898	0.364	M
<i>Trachypithecus vetellus</i>	3.847	0.385	MF
<i>Varecia variegata</i>	3.545	0.306	M
<i>Archaeolemur edwardsi</i>	4.389	0.425	M
<i>Babakotia radofilai</i>	4.21	0.307	S
<i>Hadropithecus stenognathus</i>	4.433	0.331	M
<i>Megaladapis cf madagascariensis</i>	4.58	0.291	S
<i>Megaladapis edwardsi</i>	4.877	0.306	S
<i>Mesopropithecus pithecoides</i>	3.987	0.292	S
<i>Palaeopropithecus ingens</i>	4.657	0.17	ES
<i>Elephas maximus</i>	6.538	0.439	MS
<i>Loxodonta africana</i>	6.657	0.562	MS
<i>Dendrogale murina</i>	1.653	0.075	M
<i>Ptilocercus lowii</i>	1.588	0.021	M
<i>Tupaia glis</i>	2.152	0.176	M
<i>Tupaia minor</i>	1.845	0.1	M
<i>Tupaia tana</i>	2.312	0.157	M
<i>Urogale everetti</i>	2.439	0.217	M
<i>Dugong dugon (Halicore australis)</i>	5.628	0.477	ES
<i>Bradypus tridactylus</i>	3.665	0.051	ES
<i>Bradypus variegates</i>	3.637	0.033	ES
<i>Choloepus hoffmanni</i>	3.757	0.03	ES
<i>Zaedyus pichiy</i>	3.241	0.131	MS
<i>Anomalurus derbianus</i>	2.656	0.215	F
<i>Castor canadensis</i>	4.271	0.343	M
<i>Cavia porcellus</i>	3	0.216	M
<i>Chinchilla laniger</i>	2.653	0.245	F
<i>Cryptomys hottentotus natalensis</i>	1.978	0.033	S
<i>Cryptomys mechowii</i>	2.602	0.107	S
<i>Dipus sagitta</i>	1.82	0.026	F
<i>Erethizon dorsatum</i>	4.026	0.232	S
<i>Glaucomys volans</i>	1.774	0.081	F
<i>Hydrochaeris hydrochaeris (Hydrochoerus capybara)</i>	4.597	0.419	M
<i>Idiurus macrotis</i>	1.477	-0.098	F
<i>Idiurus zenkeri</i>	1.197	-0.13	F
<i>Lophiomys imhausi</i>	2.878	0.043	S
<i>Marmota monax</i>	3.61	0.396	M
<i>Meriones unguiculatus</i>	2	0.074	M
<i>Microtus pennsylvanicus</i>	1.633	-0.081	M
<i>Mus musculus</i>	1.276	-0.257	M

<i>Myocastor coypus</i>	3.895	0.235	M
<i>Ondatra zibethicus</i>	2.998	0.235	M
<i>Pedetes capensis</i>	3.484	0.298	F
<i>Peromyscus maniculatus</i>	1.229	-0.101	M
<i>Petaurista petaurista</i>	3.267	0.322	F
<i>Rattus norvegicus</i>	2.431	0.05	M
<i>Ratufa bicolor</i>	3.138	0.317	F
<i>Ratufa macroura</i>	3.112	0.273	F
<i>Sciurus aberti</i>	2.78	0.28	F
<i>Sciurus carolinensis</i>	2.711	0.213	F
<i>Sciurus granatensis</i>	2.398	0.213	F
<i>Sciurus niger</i>	2.877	0.289	F
<i>Sciurus richmondi</i>	2.301	0.19	F
<i>Sciurus vulgaris</i>	2.507	0.183	F
<i>Spalax ehrenbergi</i>	2.23	0.117	S
<i>Spermophilus beecheyi</i>	2.791	0.205	F
<i>Spermophilus parryi</i>	2.872	0.231	F
<i>Spermophilus richardsoni</i>	2.461	0.098	F
<i>Spermophilus tridecemlineatus</i>	2.1	0.091	F
<i>Xerus erythropus</i>	2.76	0.238	F
<i>Xerus rutilus</i>	2.623	0.197	F
<i>Apodontia rufa</i>	3.1690452	0.2024202	-
<i>Sciurus carolinensis</i>	2.772725	0.2072303	-
<i>Tamiasciurus hudsonicus</i>	2.4092736	0.2354653	-
<i>Funisciurus pyrropus</i>	2.4787829	0.2369779	-
<i>Heliosciurus rufobrachium</i>	2.5502039	0.2346438	-
<i>Paraxerus cepapi</i>	2.140288	0.1271048	-
<i>Protoxerus stangeri</i>	2.8849256	0.2805215	-
<i>Aeromys tephromelas</i>	2.9564518	0.2394872	-
<i>Glaucomys volans</i>	1.8059764	0.1032905	-
<i>Petaurista petaurista</i>	3.040068	0.2861195	-
<i>Hylopetes spadiceus</i>	1.9254152	0.0442457	-
<i>Petinomys setosus</i>	1.6217992	-0.024568	-
<i>Pteromyscus pulverulentus</i>	2.2910135	0.1423112	-
<i>Pteromys buechneri</i>	2.0268192	0.1179338	-
<i>Rhinosciurus laticaudatus</i>	2.7053333	0.1728218	-
<i>Callosciurus caniceps</i>	2.6408291	0.3145519	-
<i>Lariscus insignis</i>	2.5114957	0.1669479	-
<i>Dremomys rufigenis</i>	2.6216228	0.166874	-
<i>Paramys copei</i>	3.0127908	0.1527469	-
<i>Paramys delicatus</i>	3.4644627	0.1913811	-
<i>Pseudotomus oweni</i>	3.5923667	0.1708482	-
<i>Reithroparamys delicatissimus</i>	2.9324738	0.2081053	-
<i>Rapamys atramontis</i>	2.9632837	0.2315333	-
<i>Ischyromys typus</i> ROMV 1007	3.0449355	0.1836257	-
<i>Ischyromys typus</i> AMNH F:AM 144638	3.1278269	0.1696744	-
<i>Titanotheriomys veterior</i>	2.6377528	0.1699682	-
<i>Cedromus wilsoni</i>	2.4295747	0.2021476	-
<i>Protosciurus cf. rachelae</i>	2.5435913	0.232615	-

<i>Prosciurus relictus</i>	1.4782056	0.0858255	-
<i>Mesogaulus paniensis</i>	2.4256646	0.0712374	-

For Peer Review Only

g10LSR and
without an agility
medium fast. M,

Residual

-0.068402
-0.041007
-0.049114
-0.078122
0.01201
-0.069741
-0.11904
-0.16204
-0.035924
-0.061359
-0.035656
-0.081493
-0.067826
-0.030677
-0.0068474
-0.037214
-0.11847
0.022901
-0.026627
0.0061722
-0.062319
0.048587
-0.015544
-0.01542
-0.010254
0.043618
0.052506
-0.075248
-0.076171
-0.15236
-0.0046459
-0.12776
-0.081465
-0.097661
-0.01431
-0.052626
-0.14419
0.013553
0.03078
-0.25326
-0.12879
-0.094828

For Peer Review Only

-0.19119
-0.0095758
-0.086238
-0.10057
-0.021277
-0.034423
-0.064952
-0.10492
-0.11879
0.0075684
0.005913
0.010041
-0.066619
-0.16161
-0.095502
-0.11199
-0.21919
-0.22453
-0.047686
-0.032166
-0.020051
-0.065315
-0.1868
-0.13052
-0.14546
-0.062949
0.0036817
0.085441
-0.048387
0.013946
0.016535
0.03274
0.042589
0.049592
0.074233
-0.026162
0.0395
0.020193
0.091172
0.073305
0.10021
0.09404
0.080267
0.1043
0.0073485
-0.024084
0.083815
0.06902
0.090115

For Peer Review Only

0.056024
0.089002
0.06393
0.065854
0.090572
0.1021
0.077935
0.09969
0.085481
0.06573
0.019656
0.075761
0.10748
-0.077474
0.085097
0.10219
0.09172
0.10374
0.11457
0.085699
0.087852
-0.0037336
0.048345
-0.014747
0.058234
0.11979
-0.09631
0.083305
0.068796
0.039605
0.066926
0.0042286
0.063889
0.057265
0.044529
0.026659
0.039862
0.019995
0.059755
-0.05437
0.042723
0.10123
-0.026492
-0.010549
0.076246
-0.055295
0.064741
-0.042021
0.006417

For Peer Review Only

0.081097
0.071683
0.071284
0.041839
0.07863
0.033303
0.11624
0.097785
-0.007226
0.055172
0.082908
0.043796
0.05132
-0.043037
-0.048491
-0.10791
-0.13214
-0.028583
-0.23908
-0.21852
-0.11124
0.062693
0.017278
0.097785
0.062334
0.057652
0.10088
-0.060328
-0.22705
-0.24136
-0.2602
-0.091051
0.070216
-0.015094
0.02578
0.10061
-0.022233
-0.030651
-0.0083643
-0.093734
0.052711
0.017847
-0.087061
-0.082078
-0.13111
0.12521
0.015861
-0.090665
-0.21951

For Peer Review Only

-0.073432
0.045045
0.043853
-0.057305
0.096515
-0.065066
0.10855
0.067987
0.11884
0.060952
0.10229
0.11503
0.092105
0.057896
0.028483
0.042385
0.057687
-0.021028
0.019653
0.07948
0.056575
-0.010127
0.047029
0.12327
0.1156
0.10383
0.050437
0.1055
0.055019
0.070778
0.090608
-0.004042
-0.032754
0.045735
0.056253
0.021522
0.17177
0.04125
0.026631
-0.03916255
-0.060185094
-0.097611583
0.026804158
0.046162794
-0.012529399
-0.037428948
0.02759378
0.087269394
0.102677444

For Peer Review Only

0.096604134

-0.043124335

For Peer Review Only

Table S4. Additional information for each specimen including the angle between the anterior and lateral and the posterior and lateral semicircular canals (PSC/LSC). The deviation from 90 degrees for each 90VAR for the anterior and posterior semicircular canals, and P/L 90VAR for the posterior and lateral pairs is given as 90VAR. The logarithm of the angular velocity magnitude logAVM is calculated as

	Specimen	Catalogue Number	ASC/LSC	ASC/PSC	
Fossil	<i>Paramys copei</i>	AMNH 4756	88.1	96.3	
	<i>Paramys delicatus</i>	AMNH 12506	86.6	92.6	
	<i>Pseudotomus oweni</i>	USNM 17161	77.3	90.7	
	<i>Reithroparamys delicatissimus</i>	AMNH 12561	86.7	89.1	
	<i>Rapamys atramontis</i>	AMNH 128704	85.7	85.6	
	<i>Ischyromys typus</i>	AMNH F:AM 144638	83.1	82.8	
	<i>Ischyromys typus</i>	ROMV 1007	83.6	89.7	
	<i>Titanotheriomys veterior</i>	AMNH 79314	95.6	97.4	
	<i>Cedromus wilsoni</i>	USNM 256584	87.1	82.3	
	<i>Protosciurus cf. rachelae</i>	YPM 14736	83.6	83.6	
	<i>Prosciurus relictus</i>	USNM 437793	81.8	83.8	
	<i>Mesogaulus paniensis</i>	AMNH F:AM 65511	94.1	97.8	
	Extant	<i>Aplodontia rufa</i>	AMNH 42389	88	86.2
		<i>Sciurus carolinensis</i>	AMNH 258346	85.3	82.7
<i>Tamiasciurus hudsonicus</i>		USNM 549146	84.6	83.2	
<i>Funisciurus pyrropus</i>		USNM 294865	79	82.6	
<i>Heliosciurus rufobrachium</i>		USNM 378091	88.4	83.5	
<i>Paraxerus cepapi</i>		USNM 367956	87.5	87	
<i>Protoxerus stangeri</i>		USNM 435027	76.3	81.8	
<i>Aeromys tephromelas</i>		USNM 481190	89	81.7	
<i>Glaucomyz volans</i>		AMNH 240290	78.9	86.4	
<i>Petaurista petaurista</i>		USNM 589079	80.4	85.4	
<i>Hylopetes spadiceus</i>		USNM 488639	82	82.5	
<i>Petinomys setosus</i>		USNM 488674	88.8	85.1	
<i>Pteromyscus pulverulentus</i>		USNM 481178	87.2	86.8	
<i>Pteromys buechneri</i>		USNM 172622	80.7	79.5	
<i>Rhinosciurus laticaudatus</i>		USNM 488511	80.3	88	
<i>Callosciurus caniceps</i>		USNM 294865	81	80.3	
<i>Lariscus insignis</i>		USNM 488570	89.5	81.8	
<i>Dremomys rufigenis</i>	USNM 488602	85	88.3		

ateral semicircular canals (ASC/LSC), anterior and posterior semicircular canals (ASC/PSC), h angle pair is given as A/L 90VAR for the anterior and lateral semicircular canals, A/P 90VAR for the anterior and posterior semicircular canals. The average deviation from 90 degrees for all three semicircular canal angles is given using the formula from Malinzak et al. 2012.

PSC/LSC	A/L 90VAR	A/P 90VAR	P/L 90VAR	90VAR	log90VAR	logAVM
86.5	1.9	6.3	3.5	11.7	1.068185862	2.285225211
86	3.4	2.6	4	10	1	2.32
84.1	12.7	0.7	5.9	19.3	1.285557309	2.174365772
91.9	3.3	0.9	1.9	6.1	0.785329835	2.429481784
90.5	4.3	4.4	0.5	9.2	0.963787827	2.338468208
78.6	6.9	7.2	11.4	25.5	1.40654018	2.112664508
88.8	6.4	0.3	1.2	7.9	0.897627091	2.372210183
90.7	5.6	7.4	0.7	13.7	1.136720567	2.250272511
87.8	2.9	7.7	2.2	12.8	1.10720997	2.265322915
84.9	6.4	6.4	5.1	17.9	1.252853031	2.191044954
87.3	8.2	6.2	2.7	17.1	1.23299611	2.201171984
85.6	4.1	7.8	4.4	16.3	1.212187604	2.211784322
87.2	2	3.8	2.8	8.6	0.934498451	2.35340579
85.8	4.7	7.3	4.2	16.2	1.209515015	2.213147343
79.5	5.4	6.8	10.5	22.7	1.356025857	2.138426813
84.7	11	7.4	5.3	23.7	1.374748346	2.128878344
88.3	1.6	6.5	1.7	9.8	0.991226076	2.324474701
90	2.5	3	0	5.5	0.740362689	2.452415028
88.1	13.7	8.2	1.9	23.8	1.376576957	2.127945752
83.7	1	8.3	6.3	15.6	1.193124598	2.221506455
89.6	11.1	3.6	0.4	15.1	1.178976947	2.228721757
87.8	9.6	4.6	2.2	16.4	1.214843848	2.210429637
96.4	8	7.5	6.4	21.9	1.340444115	2.146373501
88.6	1.2	4.9	1.4	7.5	0.875061263	2.383718756
88.5	2.8	3.2	1.5	7.5	0.875061263	2.383718756
97.4	9.3	10.5	7.4	27.2	1.434568904	2.098369859
89.4	9.7	2	0.6	12.3	1.089905111	2.274148393
93.7	9	9.7	3.7	22.4	1.350248018	2.141373511
89.4	0.5	8.2	0.6	9.3	0.968482949	2.336073696
90.4	5	1.7	0.4	7.1	0.851258349	2.395858242

References

- Francis CM** (2008) *A Field Guide to the Mammals of South-East Asia*. New Jersey: Princeton University Press.
- Hopkins SSB** (2005) The evolution of fossoriality and the adaptive role of horns in the Mylagaulidae (Rodentia: Caviidae). *Journal of Biogeography*, 32, 103–114.
- Hopkins SSB** (2008) Phylogeny and evolutionary history of the Aplodontioidea (Mammalia: Rodentia). *Journal of Biogeography*, 35, 103–114.
- Kingdon J** (1974). *East African mammals: an atlas of evolution in Africa*, Volume 2 part B (Hares and Rabbits). London: George Allen and Unwin.
- Nowak RM** (1999) *Walker's Mammals of the World*, Volume 2. 6th edn. Baltimore: Johns Hopkins University Press.
- Reid FA** (2006) *A Field Guide to Mammals of North America North of Mexico*, 4th edn. Boston: Houghton Mifflin Harcourt.
- Smith AT, Xie Y** (2013) *Mammals of China*. New Jersey: Princeton University Press.
- Thorington Jr RW, Koprowski JL, Steele MA, et al.** (2012) *Squirrels of the world*. Baltimore: Johns Hopkins University Press.

13.

For Peer Review Only